Journal of Network and Computer Applications 64 (2016) 43–61

Contents lists available at ScienceDirect

Journal of Network and Computer Applications

journal homepage: www.elsevier.com/locate/jnca

Reducing the energy consumption at the user equipment through multi-stream cross-carrier-aware discontinuous reception (DRX) in LTE-advanced systems

Elias Chavarria-Reyes [a,*], Etimad Fadel [b], Suleiman Almasri [b,c], M.G. Abbas Malik [b,c]

[a] Broadband Wireless Networking Laboratory, School of Electrical and Computer Engineering, Georgia Institute of Technology, Atlanta, GA 30332, USA
[b] Faculty of Computing and Information Technology, King Abdulaziz University, Jeddah, Saudi Arabia
[c] Faculty of Computing and Information Technology, University of Jeddah, Jeddah, Saudi Arabia

ARTICLE INFO

Article history:
Received 20 May 2015
Received in revised form
21 September 2015
Accepted 12 November 2015
Available online 6 February 2016

Keywords:
Discontinuous reception
DRX
Energy saving
LTE
LTE-advanced
Carrier aggregation

ABSTRACT

In order to minimize the amount of energy consumption at the user equipment (UE) level, the 3rd Generation Partnership Project (3GPP) presented in the Long Term Evolution (LTE) an approach called discontinuous reception (DRX). Nevertheless, existing models for the LTE DRX and their extension to scenarios that support carrier aggregation (CA) and multi-stream carrier aggregation (MSCA) have several drawbacks. In this paper, we utilize a semi-Markov Chain to model the operation of the LTE DRX and characterize its performance metrics. Then, we exploit the new features introduced in LTE Advanced (LTE-A) to develop a novel cross-carrier-aware DRX for scenarios that support CA and MSCA since the energy consumption in such scenarios can be significantly higher and existing techniques simply reapplied the traditional DRX scheme. We present a detailed examination of our DRX solution along with the analytical expressions of its performance metrics. The accuracy of our modeling approach for both the classical and our novel LTE DRX is validated through extensive simulations across a wide range of parameters. We evaluate the performance of our cross-carrier-aware DRX solution and show that it can significantly outperform the classical one, especially under a low tolerable delay. In addition, we also show the effects of implementation-dependent power levels on the performance of our cross-carrier-aware DRX.

1. Introduction

In addition to improving the energy efficiency of the hardware components, one of the core approaches in LTE to decreasing the energy consumption at the UE is the use of DRX (3GPP, 2013). Initially introduced by 3GPP in UMTS and later in LTE, it mainly focuses on allowing the UE to switch off most of its circuitry when no traffic is exchanged with the base station (BS). As a result, the UE can minimize the energy consumption during the "sleep" periods and maximize its on-board energy utilization. Always aware of the UE DRX state, the BS keeps the received packets while the UE is "sleeping" and sends them once the UE "awakes". The aforementioned packets undergo an additional delay, particularly detrimental in delay-sensitive traffic. Therefore, it is essential to choose the optimal values for the DRX parameters that maximize the energy savings without sacrificing the delay metrics. These values can only be optimally selected when there is a clear understanding of their impact on the DRX performance.

The performance of the LTE DRX has been previously studied in the literature, but with several simplifying assumptions that severely hinder the applicability of the results.

1. It is commonly assumed that the packet arrivals, departures, the service of a packet, and many other events can occur at any time (Zhou et al., 2008; Bontu and Illidge, 2009; Jin and Qiao, 2012). While this assumption allows for simplified formulations, it is not valid for all events. In particular, in LTE, when a packet arrives during a given subframe, it cannot be scheduled or sent during that same subframe since the scheduling grant for that subframe was previously sent during its first one to three OFDM symbols (3GPP, 2011, 2014). Therefore, such packet must wait at least until the start of the next subframe to be scheduled. Thus, the previously described assumption leads to
   - The underestimation of the time needed to empty the buffer,
   - The underestimation of the time spent waiting for a scheduling grant from the BS, and

* Corresponding author.
E-mail addresses: elias.chavarria@gatech.edu (E. Chavarria-Reyes), eafadel@kau.edu.sa (E. Fadel), smalmasri@kau.edu.sa, smalmasri@uj.edu.sa (S. Almasri), mgmalik@kau.edu.sa, mgmalik@uj.edu.sa (M.G.A. Malik).

http://dx.doi.org/10.1016/j.jnca.2015.11.022
1084-8045/

- The overestimation of the energy savings.

2. It is commonly assumed that the packet inter-arrival and service times follow an exponential distribution (Zhou et al., 2008; Bontu and Illidge, 2009; Jin and Qiao, 2012; Zhang et al., 2011; Zhou et al., 2013; Lee et al., 2013; Wang et al., 2012; Jha et al., 2013; Koc et al., 2014). As before, such assumption allows simplified formulations, but cannot be readily extended to cases where different probability distributions appear.
3. Some DRX parameters, such as the *OnDurationTimer*, have not been taken into account to simplify the formulation (Zhou et al., 2008; Bontu and Illidge, 2009; Jin and Qiao, 2012).
4. The existing literature has focused on analyzing the delay experienced by packets that arrive at the BS while the UE is "sleeping" and disregarded the effect that the buffered packets have on the ones that arrive after the "sleep" period ends. This leads to an incomplete characterization of the DRX impact on the packet delay.

With the CA and MSCA availability (Akyildiz et al., 2014), an LTE-A UE can employ up to five component carriers (CCs) simultaneously, each one of up to 20 MHz, to connect to one or more BSs. Compared to LTE, such CA consumes as much as five times more energy. In order to reduce the energy consumption, the LTE-A UE still maintains the use of DRX as the most viable option. However, the current literature on LTE-A DRX tends to follow one of the two approaches: (a) assign the same parameters to all CCs, or (b) choose a different parameter for each individual CC (Zhang et al., 2011; Zhong et al., 2011; 3GPP, 2013). The first option is simple, but inefficient and gives no flexibility, since all CCs are active, regardless of traffic transmitted. The second option does provide flexibility per CC, but lacks the cross-carrier awareness between the BS and the UE.

In this paper, we focus on mitigating the aforementioned drawbacks of the LTE-A DRX by presenting a novel solution, a cross-carrier-aware DRX. We leverage the newly introduced LTE-A features of cross-carrier resource assignment and signaling-reduced CCs. The solution we propose notably reduces the amount of energy consumed among all CCs by permitting them to enter into a "deep sleep" mode, selectively prompting their reactivation, and supporting different DRX parameters for each CC. In addition, we incorporate in our new DRX approach the current 3GPP specifications regarding the use of cross-carrier resource assignment. To develop our cross-carrier-aware DRX, we first design and analyze accurate models that address the limitations of existing modeling approaches of the classical DRX and its achievable energy savings. We build on these models to create a new one for our cross-carrier-aware DRX solution.

The rest of this paper is organized as follows. In Section 2, we introduce and analyze the operation of the LTE DRX. In particular, in Section 2.1, we describe a semi-Markov Chain model to analyze the LTE DRX. The stationary probability and the holding time of the states in such model are analyzed in Sections 2.2 and 2.3, respectively. The performance metrics are then characterized in Section 2.4. Then, we introduce our cross-carrier-aware DRX in Section 3. In particular, in Section 3.1, we present a semi-Markov Chain model to analyze our proposed solution. Then, the stationary probability and holding time of its states are analyzed in Sections 3.2–3.4, respectively. In Section 3.5, we characterize the performance metrics of our proposed DRX scheme. In Section 4, we first validate the accuracy of our analytical approach and then compare the performance of our cross-carrier-aware DRX against that of the classical DRX. Finally, we present the conclusions in Section 5.

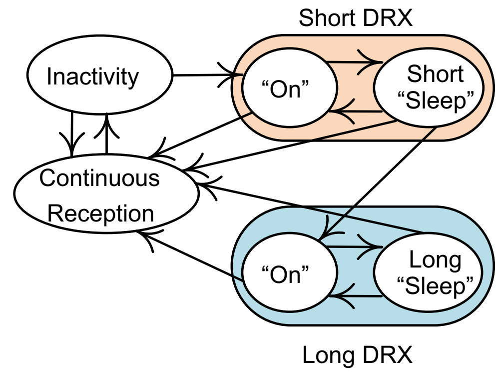

Fig. 1. LTE DRX finite state machine.

2. Classical DRX analysis

2.1. DRX model

The basic operation of DRX in LTE can be captured as a finite state machine (FSM) model, as seen in Fig. 1. While the BS is actively sending packets to the UE, the latter is in a continuous reception state (CRS). When the packet transmission from the BS is interrupted, the UE remains waiting for additional packets for a duration controlled by an inactivity timer. During this inactivity period, the UE actively monitors the physical downlink control channel (PDCCH) from the BS, looking for a scheduling grant. If the UE receives such grant before the timer expires, it returns to the CRS; otherwise, the UE starts a short DRX cycle (SDC). Such cycle is divided into two parts: an "on" period controlled by an "on" timer, and a "sleep" period. If the UE receives a scheduling grant from the BS before the "on" timer expires, it returns to the CRS. Otherwise, it transitions to the "sleep" state, where it can turn off most of its circuitry to reduce its energy consumption. The BS is always aware of the DRX parameters of the UEs; therefore, if any packet intended for a given UE arrives while that UE is in a "sleep" state, the BS buffers the packet and sends it to the UE once the latter "awakes". If no packets are awaiting at the BS for the UE by the time it "awakes", the UE starts a new SDC. While the UE receives no scheduling grant, it repeats up to N SDCs. If by the end of the N-th cycle the UE has not received a scheduling grant, it transitions to a long DRX cycle (LDC). The difference between the two cycles is the duration of the "sleep" period, which is greater in the LDC; thus, the LDC further reduces the energy consumption. The UE repeats the LDC until a scheduling grant arrives from the BS and triggers a transition to the CRS.

There are three important features in this FSM model. First, the amount of time spent in each state varies among them. For the "sleep" period, such time is fixed, while for the rest of the states it is a random variable. Second, the SDC is repeated up to N times before the LDC is reached. Thus, memory is required to track the number of SDCs previously executed. Third, it is possible to reach the CRS from every other state. However, the amount of time spent in the CRS depends directly on the previously executed state. As a result, the DRX operation cannot be directly modeled as a typical Markov Chain and requires an expansion beyond the FSM model.

We use a discrete semi-Markov Chain (SMC) with late arrival to model the DRX operation, as shown in Fig. 2. The description of each state is shown in Table 1, and the transitions are controlled by the parameters in Table 2. In a discrete late-arrival model, a packet that arrives to the BS during a given subframe x cannot be sent immediately to the UE; instead, it must wait at least for the next subframe $x+1$ to be scheduled by the BS.

We made three important considerations. First, rather than using a single state to model the continuous reception, we utilize

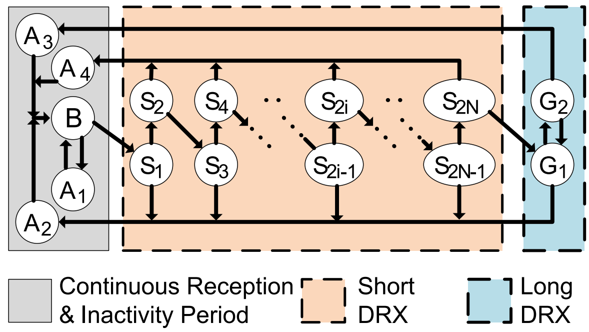

Fig. 2. LTE DRX semi-Markov Chain model.

Table 1
LTE DRX states description.

State	Description
B	Inactivity period
S_{2i}	"Sleep" period of the i-th SDC
S_{2i-1}	"On" period of the i-th SDC
G_1	"On" period of the LDC
G_2	"Sleep" period of the LDC
A_i	Continuous reception states

Table 2
LTE DRX parameters.

Parameter	Description
T_α	Inactivity period length
T_β	Short DRX cycle length
T_γ	Long DRX cycle length
N	Number of SDCs
T_{on}	"On" period length

four different states. The reasoning behind this approach is that the amount of time spent in continuous reception depends directly on the previously executed state. The four possible previously executed states are "on", "inactivity", "SDC sleep", and "LDC sleep". Second, we used A_2 to represent the CRS that follows the "on" state of the SDCs and LDCs. This is possible because the number of packets that are expected to be transmitted during continuous reception if any of these DRX cycles is interrupted during the "on" state is the same. Third, A_1 and A_2 can be merged into a single state following a similar argument as above. Nevertheless, we have chosen to avoid merging them, so we can better demonstrate the mapping between the DRX operation and the SMC model.

2.2. Stationary probability – embedded Markov Chain

Here, we present the calculation of the stationary probabilities of the embedded Markov Chain (EMC), which are required to calculate the performance metrics of the DRX.

Utilizing the notation $p_{U,U'}$ for the transition probability from state U to state U' and π_U for the stationary probability of state U in the EMC, the stationary probabilities π of the EMC follow these relationships:

$$\pi_B = \sum_{i=1}^{4} \pi_{A_i}, \quad \pi_{G_1} = \pi_{S_{2N}} p_{S_{2N},G_1} + \pi_{G_2} p_{G_2,G_1}, \tag{1a}$$

$$\pi_{G_2} = \pi_{G_1} p_{G_1,G_2}, \quad \pi_{S_1} = \pi_B p_{B,S_1}, \tag{1b}$$

$$\pi_{S_i} = \pi_{S_{i-1}} p_{S_{i-1},S_i}, \quad i \in [2,2N], \ \pi_{A_1} = \pi_B p_{B,A_1}, \tag{1c}$$

$$\pi_{A_2} = \sum_{i=1}^{N} \pi_{S_{2i-1}} p_{S_{2i-1},A_2} + \pi_{G_1} p_{G_1,A_2}, \tag{1d}$$

$$\pi_{A_3} = \pi_{G_2} p_{G_2,A_3}, \quad \pi_{A_4} = \sum_{i=1}^{N} \pi_{S_{2i}} p_{S_{2i},A_4}. \tag{1e}$$

From these expressions we obtain

$$\pi_B = \frac{\phi}{p_{B,S_1}}, \quad \pi_{G_1} = \phi\omega\theta, \quad \pi_{G_2} = \phi\omega\theta p_{G_1,G_2}, \tag{2a}$$

$$\pi_{S_1} = \phi, \quad \pi_{S_i} = \phi \prod_{j=2}^{i} p_{S_{j-1},S_j}, \ i \in [2,2N], \tag{2b}$$

$$\pi_{A_1} = \phi \frac{p_{B,A_1}}{p_{B,S_1}}, \quad \pi_{A_3} = \phi\omega\theta p_{G_1,G_2} p_{G_2,A_3}, \tag{2c}$$

$$\pi_{A_2} = \phi\left[p_{S_1,A_2} + \omega\theta p_{G_1,A_2} + \sum_{i=2}^{N}\left(p_{S_{2i-1},A_2} \prod_{j=2}^{2i-1} p_{S_{j-1},S_j}\right)\right], \tag{2d}$$

$$\pi_{A_4} = \phi \sum_{i=1}^{N}\left(p_{S_{2i},A_4} \prod_{j=2}^{2i} p_{S_{j-1},S_j}\right), \tag{2e}$$

where

$$\omega = p_{S_{2N},G_1} \prod_{j=2}^{2N} p_{S_{j-1},S_j}, \quad \theta = (1 - p_{G_1,G_2} p_{G_2,G_1})^{-1}. \tag{3}$$

With these expressions, the value of ϕ becomes

$$\phi = \left[1 + \frac{2}{p_{B,S_1}} + \omega\theta(1 + p_{G_1,G_2}) + \sum_{i=2}^{2N} \prod_{j=2}^{i} p_{S_{j-1},S_j}\right]^{-1}, \tag{4}$$

which can be plugged into Eq. (2) to obtain the stationary probabilities of all the states of the EMC model.

To find the actual values of the above expressions, we need the transition probabilities, which depend on the BS packet arrival model, probability distribution, and the service discipline. For the latter, we consider that the BS has a separate and infinite buffer for each UE, a common assumption in the existing literature. Thus, the rest of the analysis focuses on the DRX operation for a single UE. For the packet arrival model, we utilize a late-arrival model (Takagi, 1993). For the packet arrival distribution, we consider that the number of packets that arrive at the BS during successive subframes constitutes a sequence of independent and identically distributed (i.i.d.) random variables. Considering such distribution to be i.i.d. allows us to capture a wider range of scenarios than just considering an exponential inter-arrival time. We use Λ to denote the number of packets that arrive in one subframe. The probability mass function (PMF) of Λ is defined as

$$\lambda(k) \triangleq \text{Prob}\{\Lambda = k\}, \quad k = 0, 1, 2\ldots, \tag{5}$$

and its mean value is defined as $\lambda \triangleq E\{\Lambda\}$, where $E\{\Lambda\}$ denotes the expected value of Λ. We denote as X the service time (in subframes units) of a single packet; its PMF is defined as

$$b(l) = \text{Prob}\{X = l\}, \quad l = 1, 2, \ldots, \tag{6}$$

and its mean value is defined as $b \triangleq E\{X\}$.

Having the arrival model, the service discipline, and the PMF of the packet arrivals and the service time, we proceed to characterize the transition probabilities. To achieve this, we (a) apply the conditions that trigger each transition, as described in Section 2.1, and (b) consider that the probability of a BS receiving no packets in a time period of length ν is equal to $[\lambda(0)]^\nu$ since the number of packet arrivals in successive subframes constitutes a sequence of i.i.d. random variables. Hence, the probability that the BS receives at least one packet in a time period of length ν is equal to $1-[\lambda(0)]^{\nu}$:

$$p_{B,S_1}=[\lambda(0)]^{T_\alpha},\quad p_{B,A_1}=1-p_{B,S_1}, \tag{7a}$$

$$p_{S_{2i-1},S_{2i}}=[\lambda(0)]^{T_{\rm on}-1},\quad i\in[1,N], \tag{7b}$$

$$p_{S_{2i-1},A_2}=1-p_{S_{2i-1},S_{2i}},\quad i\in[1,N], \tag{7c}$$

$$p_{S_{2i},S_{2i+1}}=[\lambda(0)]^{T_\beta-T_{\rm on}+1},\quad i\in[1,N-1], \tag{7d}$$

$$p_{S_{2i},A_4}=1-[\lambda(0)]^{T_\beta-T_{\rm on}+1},\quad i\in[1,N], \tag{7e}$$

$$p_{S_{2N},G_1}=[\lambda(0)]^{T_\beta-T_{\rm on}+1}, \tag{7f}$$

$$p_{G_1,G_2}=[\lambda(0)]^{T_{\rm on}-1},\quad p_{G_1,A_2}=1-p_{G_1,G_2}, \tag{7g}$$

$$p_{G_2,G_1}=[\lambda(0)]^{T_\gamma-T_{\rm on}+1},\quad p_{G_2,A_3}=1-p_{G_2,G_1}. \tag{7h}$$

Having the transition probabilities, we plug them into Eqs. (3) and (4) and obtain

$$\phi=\left[\frac{2}{[\lambda(0)]^{T_\alpha}}+\left(1+[\lambda(0)]^{T_{\rm on}-1}\right)\left(\frac{1-[\lambda(0)]^{NT_\beta}}{1-[\lambda(0))^{T_\beta}}+\frac{[\lambda(0)]^{NT_\beta}}{1-[\lambda(0)]^{T_\gamma}}\right)\right]^{-1}. \tag{8}$$

Then, the stationary probabilities for the EMC become

$$\pi_B=\frac{\phi}{[\lambda(0)]^{T_\alpha}}, \tag{9a}$$

$$\pi_{S_i}=\phi\begin{cases}[\lambda(0)]^{T_\beta(i-1)/2} & : i \text{ is odd}\\ [\lambda(0)]^{T_\beta(i-2)/2}[\lambda(0)]^{T_{\rm on}-1} & : i \text{ is even}\end{cases}, i\in[1,2N], \tag{9b}$$

$$\pi_{G_1}=\phi\frac{[\lambda(0)]^{NT_\beta}}{1-[\lambda(0)]^{T_\gamma}},\quad \pi_{G_2}=\pi_{G_1}[\lambda(0)]^{T_{\rm on}-1}, \tag{9c}$$

$$\pi_{A_1}=\phi\left(\frac{1}{[\lambda(0)]^{T_\alpha}}-1\right), \tag{9d}$$

$$\pi_{A_2}=\phi\left(1-[\lambda(0)]^{T_{\rm on}-1}\right)\left(\frac{1-[\lambda(0)]^{NT_\beta}}{1-[\lambda(0)]^{T_\beta}}+\frac{[\lambda(0)]^{NT_\beta}}{1-[\lambda(0)]^{T_\gamma}}\right), \tag{9e}$$

$$\pi_{A_3}=\phi[\lambda(0)]^{NT_\beta}\left[1-\frac{1-[\lambda(0)]^{T_{\rm on}-1}}{1-[\lambda(0)]^{T_\gamma}}\right], \tag{9f}$$

$$\pi_{A_4}=\phi\left[1-[\lambda(0)]^{NT_\beta}\right]\left[1-\frac{1-[\lambda(0)]^{T_{\rm on}-1}}{1-[\lambda(0)]^{T_\beta}}\right]. \tag{9g}$$

In addition to the stationary probabilities of the EMC, the mean amount of time spent in each state is also needed to compute the performance metrics.

2.3. Holding time

The holding time H_U of a state U represents the mean amount of time spent in such state. The states corresponding to "sleep" periods have a deterministic holding time, since the length of the "sleep" periods is a constant:

$$H_{S_{2i}}=T_\beta-T_{\rm on},\quad i\in[1,N], \tag{10a}$$

$$H_{G_2}=T_\gamma-T_{\rm on}. \tag{10b}$$

The holding time of the "on" periods and the inactivity period can be calculated as follows. Consider the maximum length of any such period to be equal to ν, and the amount of time spent in it to be L. Then, the PMF of L is

$$\text{Prob}\{L=i|\nu\}=\begin{cases}[\lambda(0)]^{i-1}(1-\lambda(0)) & : 0<i<\nu\\ [\lambda(0)]^{\nu-1} & : i=\nu\end{cases}, \tag{11}$$

i.e., $L=i, i<\nu$, if no packets are received in the first $i-1$ subframes and at least one packet arrives during the i-th subframe. $L=\nu$ if no packets arrived during the previous $\nu-1$ subframes, regardless of whether a packet arrives in the last subframe or not. Taking the expected value of L, we obtain:

$$H=E\{L|\nu\}=\frac{1-[\lambda(0)]^{\nu}}{1-\lambda(0)}. \tag{12}$$

For the "on" periods, $\nu=T_{\rm on}$ and for the inactivity period, $\nu=T_\alpha$. Hence,

$$H_{S_{2i-1}}=E\{L|\nu=T_{\rm on}\}=\frac{1-[\lambda(0)]^{T_{\rm on}}}{1-\lambda(0)},\quad i\in[1,N], \tag{13a}$$

$$H_{G_1}=E\{L|\nu=T_{\rm on}\}=\frac{1-[\lambda(0)]^{T_{\rm on}}}{1-\lambda(0)}, \tag{13b}$$

$$H_B=E\{L|\nu=T_\alpha\}=\frac{1-[\lambda(0)]^{T_\alpha}}{1-\lambda(0)}. \tag{13c}$$

States A_1 through A_4 correspond to a busy period in queuing theory terminology (Takagi, 1993), from which it follows that if a busy period A starts with R_A packets in the buffer, its duration L has a mean value of

$$E\{L|R_A\}=R_A\frac{b}{1-\rho}, \tag{14}$$

where $\rho=b\lambda$. Thus, applying the law of total expectation,

$$E\{L\}=E\{\{L|R_A\}\}=E\{R_A\}\frac{b}{1-\rho}. \tag{15}$$

$$\begin{aligned}\Psi=&\frac{1-[\lambda(0)]^{NT_\beta}}{1-[\lambda(0)]^{T_\beta}}\Big[H_{S_1}+H_{S_2}[\lambda(0)]^{T_{\rm on}-1}\\ &+(H_{A_2}-H_{A_4})\left(1-[\lambda(0)]^{T_{\rm on}-1}\right)\Big]+[\lambda(0)]^{NT_\beta}H_{A_3}\\ &+\left(1-[\lambda(0)]^{NT_\beta}\right)H_{A_4}+\frac{[\lambda(0)]^{NT_\beta}}{1-[\lambda(0)]^{T_\gamma}}\Big[H_{G_1}+H_{G_2}[\lambda(0)]^{T_{\rm on}-1}\\ &+(H_{A_2}-H_{A_3})\left(1-[\lambda(0)]^{T_{\rm on}-1}\right)\Big]+\frac{H_B+\left(1-[\lambda(0)]^{T_\alpha}\right)H_{A_1}}{[\lambda(0)]^{T_\alpha}}.\end{aligned} \tag{16}$$

Hence, to obtain the holding time of the states $A_i, i\in[1,4]$ we need the expected value of the number of packets in the BS buffer when each state starts. This quantity can be obtained as follows. Consider F to be the number of packets received by the BS during time ν, and Q to denote F conditioned on at least one packet arrival. As a result,

$$\text{Prob}\{Q=k|\nu\}=\begin{cases}\dfrac{\text{Prob}\{F=k|\nu\}}{1-\text{Prob}\{F=0|\nu\}} & : k>0\\ 0 & : k=0\end{cases}, \tag{17a}$$

$$E\{Q|\nu\}=\frac{E\{F|\nu\}}{1-\text{Prob}\{F=0|\nu\}}. \tag{17b}$$

Since F is the sum of ν random variables Λ, $E\{F|\nu\}=\nu E\{\Lambda\}=\nu\lambda$. In addition, $\text{Prob}\{F=0|\nu\}=[\lambda(0)]^{\nu}$ since it represents the probability of no packet arrival in ν subframes. With the previous expressions, we obtain

$$E\{Q|\nu\}=\lambda\frac{\nu}{1-[\lambda(0)]^{\nu}}. \tag{18}$$

$E\{Q\,|\,\nu\}$ represents the expected number of packets buffered at the BS after ν subframes, given that at least one packet arrives. This expression allows us to obtain R_{A_i} for each state A_i since each one is entered when the BS has received at least one packet during a given number of previous subframes. Specifically, $E\{R_{A_1}\} = E\{R_{A_2}\} = E\{Q\,|\,\nu = 1\}$, $E\{R_{A_3}\} = E\{Q\,|\,\nu = T_\gamma - T_{\text{on}} + 1\}$, and $E\{R_{A_4}\} = E\{Q\,|\,\nu = T_\beta - T_{\text{on}} + 1\}$. Hence, the holding times of A_1, A_2, A_3, and A_4 are, respectively,

$$H_{A_1} = E\{R_{A_1}\}\frac{b}{1-\rho} = \frac{\rho}{1-\rho}\frac{1}{1-[\lambda(0)]}, \tag{19a}$$

$$H_{A_2} = E\{R_{A_2}\}\frac{b}{1-\rho} = \frac{\rho}{1-\rho}\frac{1}{1-[\lambda(0)]}, \tag{19b}$$

$$H_{A_3} = E\{R_{A_3}\}\frac{b}{1-\rho} = \frac{\rho}{1-\rho}\frac{T_\gamma - T_{\text{on}} + 1}{1-[\lambda(0)]^{T_\gamma - T_{\text{on}} + 1}}, \tag{19c}$$

$$H_{A_4} = E\{R_{A_4}\}\frac{b}{1-\rho} = \frac{\rho}{1-\rho}\frac{T_\beta - T_{\text{on}} + 1}{1-[\lambda(0)]^{T_\beta - T_{\text{on}} + 1}}. \tag{19d}$$

Having the holding time of each state, we proceed to obtain the performance metrics.

2.4. Performance metrics

The two main performance metrics associated with DRX are the amount of energy saved and the packet delay.

2.4.1. Energy savings

In general, the energy savings depend on the amount of time spent in the "sleep" and "non-sleep" periods and the respective amount of power consumed during each one. Since the latter depends on the actual implementation, in our work we utilize the amount of time spent in the "sleep period" as an implementation-independent proxy metric for the energy savings. This value is obtained from the stationary probabilities of the SMC, which we derive from the stationary probabilities of the EMC, Eqs. (9a)–(9f).

For any state U, whose stationary probability in the EMC is π_U and whose holding time is H_U, the stationary probability $\tilde{\pi}_U$ in the SMC is

$$\tilde{\pi}_U = \frac{\pi_U H_U}{\sum_{\forall U'} \pi_{U'} H_{U'}}. \tag{20}$$

Then, the energy savings τ_β and τ_γ provided by the short and long DRX, respectively, are

$$\tau_\beta = \sum_{i=1}^{N} \tilde{\pi}_{S_{2i}}, \quad \tau_\gamma = \tilde{\pi}_{G_2}. \tag{21}$$

Replacing the expressions for the holding time and the stationary probabilities of the EMC, τ_β and τ_γ become

$$\tau_\beta = \frac{1}{\Psi}(T_\beta - T_{\text{on}})\frac{1-[\lambda(0)]^{NT_\beta}}{1-[\lambda(0)]^{T_\beta}}[\lambda(0)]^{T_{\text{on}}-1}, \tag{22a}$$

$$\tau_\gamma = \frac{1}{\Psi}(T_\gamma - T_{\text{on}})\frac{[\lambda(0)]^{NT_\beta}}{1-[\lambda(0)]^{T_\gamma}}[\lambda(0)]^{T_{\text{on}}-1}, \tag{22b}$$

where Ψ is expressed in Eq. (16). Then, the total energy savings τ become

$$\tau = \tau_\beta + \tau_\gamma. \tag{23}$$

If in a given implementation, the power consumption during the "non-sleep" and "sleep" states are $P_{\max}$ and $c_0 P_{\max}$ $(0 \le c_0 \le 1)$, respectively, then the implementation-dependent energy savings are

$$(1-c_0)\tau. \tag{24}$$

2.4.2. Delay

To calculate the expected value $E\{\Gamma\}$ of the packet delay, also called waiting time in queuing theory terminology, we need to compute (a) the expected value of the delay W_i, $i \in [1,4]$ experienced by the packets sent in A_i, $i \in [1,4]$, and (b) the probability of a packet being sent in each of those states. To compute the delay, we utilize the results from queuing theory establishing the expected value $E\{W\}$ of the packet waiting time in a system with vacation (Takagi, 1993). In such context,

$$E\{W\,|\,\nu\} = \frac{\lambda^2 E\{X^2\} + bE\{\Lambda^2\} - \rho(\lambda+1)}{2\lambda(1-\rho)} + \frac{E\{\nu(\nu-1)\}}{2E\{\nu\}}, \tag{25}$$

where ν is the length of the vacation, the first term represents the waiting time in a system without vacation, and the second term represents the residual life of the vacation time. In the context of DRX, ν corresponds to the amount of time during which the BS buffers packets before entering a CRS. Therefore, ν is a deterministic value equal to 1 for A_1 and A_2, $T_\gamma - T_{\text{on}} + 1$ for A_3, and $T_\beta - T_{\text{on}} + 1$ for A_4. It then follows that

$$E\{W_1\} = E\{W_2\} = \frac{\lambda^2 E\{X^2\} + bE\{\Lambda^2\} - \rho(\lambda+1)}{2\lambda(1-\rho)}, \tag{26a}$$

$$E\{W_3\} = E\{W_1\} + \frac{T_\gamma - T_{\text{on}}}{2}, \tag{26b}$$

$$E\{W_4\} = E\{W_1\} + \frac{T_\beta - T_{\text{on}}}{2}. \tag{26c}$$

We now proceed to compute the probability of a packet being sent from state A_i. First, we denote by $\hat{R}_{A_i}$ the number of packets sent during A_i. By Little's theorem,

$$E\left\{\hat{R}_{A_i}\right\} = \frac{H_{A_i}}{b}. \tag{27}$$

Then, the probability of a packet being sent from A_i is

$$\text{Prob}\{Y = A_i\} = \frac{\pi_{A_i} E\{\hat{R}_{A_i}\}}{\sum_{j=1}^{4} \pi_{A_j} E\{\hat{R}_{A_j}\}} = \frac{\pi_{A_i} H_{A_i}}{\sum_{j=1}^{4} \pi_{A_j} H_{A_j}}, \tag{28}$$

where Y denotes the state from which the packet is sent. Now, applying the law of total expectation, we have that

$$\begin{aligned} E\{\Gamma\} = E\{E\{\Gamma\,|\,Y\}\} &= \sum_{i=1}^{4} E\{\Gamma\,|\,Y = A_i\}\text{Prob}\{Y = A_i\} \\ &= \sum_{i=1}^{4} E\{W_i\}\text{Prob}\{Y = A_i\}. \end{aligned} \tag{29}$$

After further simplification, the above expression becomes

$$E\{\Gamma\} = E\{W_1\} + \frac{(T_\gamma - T_{\text{on}})\pi_{A_3} E\{H_{A_3}\} + (T_\beta - T_{\text{on}})\pi_{A_4} E\{H_{A_4}\}}{2\sum_{j=1}^{4} \pi_{A_j} E\{H_{A_j}\}}. \tag{30}$$

As mentioned previously, the first term represents the waiting time in a system with no vacation/DRX. Hence, the second term denotes the additional waiting time caused by the use of DRX.

3. Cross-carrier-aware DRX analysis

In a scenario supporting CA or MSCA, the cell that handles the radio resource control connection (3GPP, 2014) is called the primary cell (PCell), which is served by a primary component carrier. If a UE supports multiple CCs, then secondary cells (SCells) can be added to the user's set of serving cells. The cross-carrier awareness arises from the fact that the medium access control (MAC) (3GPP,

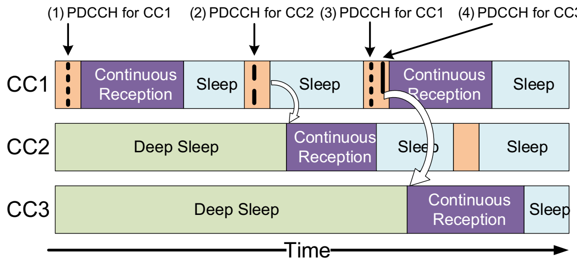

Fig. 3. Cross-carrier-aware DRX operation.

2013) is exposed to the multi-CC nature of the physical layer, even though the radio link control (3GPP, 2010) and the packet data convergence protocol (3GPP, 2013) are unaware of such nature. To exploit the cross-carrier awareness, we employ the same- and cross-carrier scheduling methods supported at the MAC layer. The same-carrier method corresponds to the scheme used for LTE. The cross-carrier method allows the BS to use a particular CC to assign resources contained in a different CC. However, there are certain restrictions. First, only the PCell schedules its resources. It does so through the PDCCH. Second, cross-carrier scheduling only applies when the PDCCH of an SCell is not configured. As a result, a CC whose resources are allocated through cross-carrier scheduling cannot have its own DRX parameters. Conversely, a CC that has its own PDCCH and, therefore, its own DRX parameters, cannot be scheduled by the PCell through cross-carrier scheduling. We now describe our cross-carrier-aware DRX that accounts for the aforementioned constraints and provides improved performance compared to the traditional DRX.

The basic concepts behind our cross-carrier-aware DRX are captured in Fig. 3, which depicts the operation of a UE with three CCs, where CC1 represents the PCell as an anchor CC and the rest of CCs as SCells.

Event 1. At the UE, the anchor CC receives a PDCCH indicating that the upcoming subframes in CC1 contain data. Following the traditional DRX behavior, CC1 enters a CRS until no more data is received and then returns to “sleep”. While CC1 performs the aforementioned steps, CC2 and CC3 remain in a “deep sleep” state (DSS) since no data has arrived for them. In contrast to the traditional LTE DRX “sleep states”, the DSS in our proposed solution does not require CC2 and CC3 to “wake up” to check if a PDCCH has arrived. Thus, our solution has a greater potential to save energy.

Event 2. Similar to the concept of cross-carrier scheduling, we propose the use of a cross-carrier DRX activation. For example, once the UE “wakes up” its anchor CC to listen for the presence of a PDCCH, such UE identifies whether a PDCCH indicates subsequent data in the anchor CC or in an SCell. In event 2, the PDCCH indicates subsequent data in CC2. Therefore, the UE “wakes up” CC2 from the DSS so that it can receive the upcoming data, while allowing CC1 to go back to its normal “sleep” state. Because of the synchronization and timing differences between CC1 and CC2, the activation of the latter is delayed, and so is the packet reception. This delay is the penalty that our system incurs for providing the energy savings of the DSS. In event 2, we also observe that the proposed cross-carrier activation is selective, e.g., only CC2 is activated, leaving CC3 in the DSS. Another feature of our proposed solution is the ability to set per-carrier DRX parameters. For example, once CC2 is activated as a result of event 2, we allow for CC2 to utilize its own DRX parameters, which may be completely different from the ones of CC1, and thus can be optimized to the characteristics of the traffic carried over CC2.

Events 3 *and* 4. At the UE, the anchor CC receives two PDCCH. The first and second PDCCH indicate that the upcoming subframes in CC1 and CC3, respectively, contain data. Therefore, both CCs then enter a CRS. We observe that the operation of CC2 is not affected by the DRX events of CC1 since at this point CC2 is following its own DRX parameters. As in event 2, once CC3 enters the CRS, it follows its own DRX parameters, which can be different from the ones of CC1 and CC2.

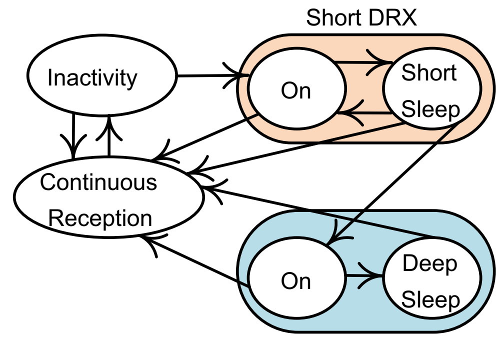

Fig. 4. Cross-carrier-aware DRX finite state machine for SCell.

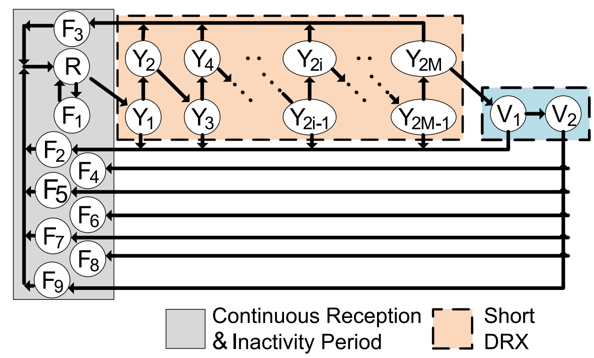

Fig. 5. Cross-carrier-aware DRX semi-Markov Chain model for SCell.

3.1. Cross-carrier-aware DRX model

As previously described, the anchor CC in our proposed cross-carrier-aware DRX follows the traditional LTE DRX operation and supports the cross-carrier-aware DRX operation of the SCells. Such support does not affect the DRX operation of the anchor; therefore, its analysis and performance metrics correspond to the ones presented in Section 2. In this section, we focus on the analysis of the cross-carrier-aware DRX operation of a single SCell. Such operation is captured as a finite state machine (FSM) model in Fig. 4. Compared to the FSM of the traditional LTE DRX, depicted in Fig. 1, the one in Fig. 4 does not have an LDC that may be repeated any number of times; instead, it has a single entrance to the DSS and a subsequent exit only to the CRS. The exit transition from the DSS is triggered by the events occurring at the anchor CC.

As discussed in Section 2.1, the DRX operation cannot be directly modeled as a typical Markov Chain using the FSM of Fig. 4. We use an SMC with late arrival to model the cross-carrier-aware DRX operation of the SCell, as shown in Fig. 5. The description of each state is shown in Table 3. Even though the DSS is represented in Fig. 5 as a single state V_2, it encompasses a group of states that captures the events occurring at the anchor while the SCell is in the DSS.

Rather than using a single state to model the continuous reception, we utilize nine different states. The reason for this approach is that the amount of time spent in continuous reception depends on the SCell state at the moment that the packet triggering the continuous reception arrives at the BS. $F_i, i \in [1,3]$ are used when such packet arrives when the SCell is in the “inactivity”, “on”, and SDC “sleep” state, respectively. From Fig. 5, we also observe that state V_2 leads to each of the five CRSs $F_i, i \in [4,9]$. This

Table 3
Cross-carrier-aware DRX states description.

State	Description
R	Inactivity period
Y_{2i} $i \in [1, M]$	"Sleep" period of the i-th SDC
Y_{2i-1} $i \in [1, M]$	"On" period of the i-th SDC
V_1	"On" period preceding the DSS
V_2	DSS
F_i $i \in [1, 9]$	Continuous reception states

Table 4
Cross-carrier-aware DRX parameters for the SCell.

Parameter	Description
$T_{\alpha 2}$	Inactivity period length
$T_{\beta 2}$	Short DRX cycle length
M	Number of SDCs
$T_{\text{on}2}$	"On" period length

Table 5
Cross-carrier-aware DRX parameters for the anchor CC.

Parameter	Description
T_{α_1}	Inactivity period length
T_{β_1}	Short DRX cycle length
T_{γ_1}	Long DRX cycle length
N	Number of SDCs
$T_{\text{on}1}$	"On" period length

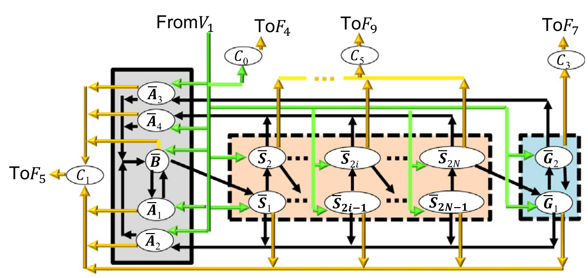

Fig. 6. Internal semi-Markov Chain of the DSS.

occurs because V_2 encompasses multiple internal states, each of which may produce a different number of packets that need to be sent in a CRS. The internal states of V_2 and how they lead to $F_i, i \in [4, 9]$ will be later discussed in this section.

Except for the ones exiting the DSS, all the transitions in Fig. 5 are controlled by the parameters in Table 4 and reflect the DRX operation described in Section 3. Therefore, the same events that trigger a transition in the traditional LTE DRX (Section 2.1) determine the transitions (i) from the CRSs to the inactivity state and vice versa, (ii) within the SDCs, (iii) from the SDCs to the CRSs, and (iv) from Y_{2M} to the next "on" period. The transitions that exit the DSS V_2 are controlled by the events occurring at the anchor CC and its DRX parameters, which are shown in Table 5.[1]

Once the SCell enters the DSS, the UE starts tracking the events of the anchor CC waiting for a PDCCH indicating that the BS has a packet ready for the SCell, i.e., entering the DSS is equivalent to

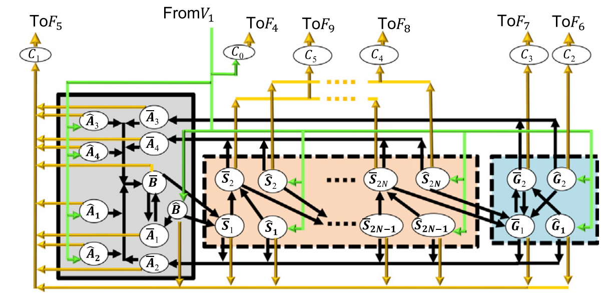

Fig. 7. Internal semi-Markov Chain of the DSS with synchronization states.

starting the SMC of the anchor CC from a randomly selected state, as shown in Fig. 6. There, the states of the form $\overline{U}$ represent the ones being tracked at the anchor CC. States $C_i, i \in \{0, 1, 3, 5\}$, capture the ones executed after the anchor CC receives a PDCCH indicating that the BS has a packet for the SCell. After any such state is executed, the DSS ends, and the SCell transitions to a CRS F_i.

When the SCell transitions from V_1 to V_2, not only the anchor CC is executing a randomly selected state, but also the amount of time left until the end of such state is a random variable. For example, when the SCell enters the DSS, it may occur that the anchor CC is in the middle of a "sleep" period of a SDC rather than at the beginning of such period. For this reason, when the SCell enters the DSS, it needs to synchronize with the anchor CC to account for the randomness in the amount of time left until the end of the landed state. Such synchronization is captured in Fig. 7 by introducing the states of the form $\hat{U}$. States C_2 and C_4 are also added to account for the possibility of exiting the DSS during or immediately after a synchronization state associated with a "sleep" state.

In Fig. 7, C_0 has a key role in the transition probabilities from V_1 to the synchronization states. C_0 reflects a packet arriving at the BS for the SCell during the last subframe x of V_1, i.e., when the transition to the DSS is inevitable. Since that packet cannot be sent during subframe x, it must wait at least for the next subframe $x+1$. If during subframe $x+1$ the anchor is in a non-"sleep" state, then the BS can notify the UE in that same subframe that it has a packet for the SCell; therefore, the SCell should exit the DSS. This scenario is the one captured by state C_0. As a result, the only cases where a synchronization state is reached are the ones where no packet arrived to the BS for the SCell during the last subframe x of V_1, or where the anchor CC is in a "sleep" state during subframe $x+1$.

3.2. Stationary probability – embedded Markov Chain – SCell

In this section, we present the calculation of the stationary probability of the EMC corresponding to the SMC in Fig. 5.

Utilizing the same notation of Section 2.2, the stationary probabilities π of the EMC follow these relationships:

$$\pi_R = \sum_{i=1}^{9} \pi_{F_i}, \quad \pi_{Y_1} = \pi_R p_{R,Y_1}, \tag{31a}$$

$$\pi_{Y_i} = \pi_{Y_{i-1}} p_{Y_{i-1},Y_i}, \quad i \in [2, 2M], \tag{31b}$$

$$\pi_{V_1} = \pi_{Y_{2M}} p_{Y_{2M},V_1}, \quad \pi_{V_2} \triangleq \sum_{\forall U \in V_2} \pi_U, \tag{31c}$$

$$\pi_{F_1} = \pi_R p_{R,F_1}, \quad \pi_{F_3} = \sum_{i=1}^{M} \pi_{Y_{2i}} p_{Y_{2i},F_3}, \tag{31d}$$

$$\pi_{F_2} = \sum_{i=1}^{M} \pi_{Y_{2i-1}} p_{Y_{2i-1},F_2} + \pi_{V_1} p_{V_1,F_2}. \tag{31e}$$

[1] The parameters in Table 5 are equivalent to the ones in Table 2. Here, the notation has been adjusted to facilitate the differentiation of the parameters of the anchor CC from the ones of the SCell.

From these expressions we obtain:

$$\pi_{F_1} = \phi_2 \frac{p_{R,F_1}}{p_{R,Y_1}}, \quad \pi_{F_3} = \phi_2 \sum_{i=1}^{M} \left(p_{Y_{2i},F_3} \prod_{j=2}^{2i} p_{Y_{j-1},Y_j} \right), \tag{32a}$$

$$\pi_{F_2} = \phi_2 \left[p_{Y_1,F_2} + \omega_2 p_{V_1,F_2} + \sum_{i=2}^{M} \left(p_{Y_{2i-1},F_2} \prod_{j=2}^{2i-1} p_{Y_{j-1},Y_j} \right) \right], \tag{32b}$$

$$\pi_{V_1} = \phi_2 \omega_2, \quad \pi_{V_2} = \phi_2 \omega_2 \omega_3, \quad \pi_{Y_1} = \phi_2 \tag{32c}$$

$$\pi_{Y_i} = \phi_2 \prod_{j=2}^{i} p_{Y_{j-1},Y_j}, \; i \in [2, 2M], \quad \pi_R = \frac{\phi_2}{p_{R,Y_1}}, \tag{32d}$$

where

$$\omega_2 = p_{Y_{2M},V_1} \prod_{j=2}^{2M} p_{Y_{j-1},Y_j}, \quad \omega_3 = \sum_{\forall U \in V_2} \frac{\pi_U}{\pi_{V_1}}. \tag{33}$$

With these expressions, the value of ϕ_2 becomes

$$\phi_2 = \left[1 + \frac{2}{p_{R,Y_1}} + \omega_2(1+\omega_3) + \sum_{i=2}^{2M} \prod_{j=2}^{i} p_{Y_{j-1},Y_j} \right]^{-1}, \tag{34}$$

which can be plugged into Eq. (32) to obtain the stationary probabilities of all the states of the EMC model.

As in Section 2.2, we utilize a late-arrival model for the packet arrival in the SCell. We utilize Λ_2 to denote the number of packets that arrive in a single subframe. The PMF of Λ_2 is defined as

$$\lambda_2(k) \triangleq \text{Prob}\{\Lambda_2 = k\}, \quad k = 0, 1, 2\ldots, \tag{35}$$

and its mean value is defined as $\lambda_2 \triangleq E\{\Lambda_2\}$. We denote as X_2 the service time of a single packet in the SCell. The PMF of X_2 is defined as

$$b_2(l) = \text{Prob}\{X_2 = l\}, \quad l = 1, 2, \ldots, \tag{36}$$

and its mean value is defined as $b_2 \triangleq E\{X_2\}$.

Having the arrival model, the service discipline, and the PMF of the packet arrivals and the service time, we proceed to characterize the transition probabilities. To achieve this, we (a) apply the conditions that trigger each transition, as described in Section 3.1, and (b) consider that the probability of a BS receiving no packets in a time period of length ν is equal to $[\lambda_2(0)]^{\nu}$ since the number of packet arrivals in successive subframes constitutes a sequence of i.i.d. random variables. Hence, the probability that the BS receives at least one packet in a time period of length ν is equal to $1-[\lambda_2(0)]^{\nu}$.

$$p_{R,Y_1} = [\lambda_2(0)]^{T_{\alpha 2}}, \quad p_{R,F_1} = 1 - p_{R,Y_1}, \tag{37a}$$

$$p_{Y_{2i-1},Y_{2i}} = [\lambda_2(0)]^{T_{\text{on2}}-1}, \quad i \in [1, M], \tag{37b}$$

$$p_{Y_{2i-1},F_2} = 1 - p_{Y_{2i-1},Y_{2i}}, \quad i \in [1, M], \tag{37c}$$

$$p_{Y_{2i},Y_{2i+1}} = [\lambda_2(0)]^{T_{\beta 2}-T_{\text{on2}}+1}, \quad i \in [1, M-1], \tag{37d}$$

$$p_{Y_{2i},F_3} = 1 - [\lambda_2(0)]^{T_{\beta 2}-T_{\text{on2}}+1}, \quad i \in [1, M], \tag{37e}$$

$$p_{Y_{2M},V_1} = [\lambda_2(0)]^{T_{\beta 2}-T_{\text{on2}}+1}, \tag{37f}$$

$$p_{V_1,F_2} = 1 - [\lambda_2(0)]^{T_{\text{on2}}-1}, \tag{37g}$$

$$p_{V_1,V_2} \triangleq \sum_{\forall U \in V_2} p_{V_1,U} = [\lambda_2(0)]^{T_{\text{on2}}-1}, \tag{37h}$$

where p_{V_1,V_2} is not a real transition probability since V_2 represents a group of states, but the probability of going from V_1 to any of the states that belong to V_2. Having the above transition probabilities, we plug them into Eqs. (32) and (33) and obtain

$$\phi_2 = \left[\frac{2}{[\lambda_2(0)]^{T_{\alpha 2}}} + \left(1 + [\lambda_2(0)]^{T_{\text{on2}}-1}\right) \left(\frac{1-[\lambda_2(0)]^{MT_{\beta 2}}}{1-[\lambda_2(0)]^{T_{\beta 2}}} \right) + (1+\omega_3)[\lambda_2(0)]^{MT_{\beta 2}} \right]^{-1}. \tag{38}$$

Then, the stationary probabilities for the EMC become

$$\pi_R = \frac{\phi_2}{[\lambda(0)]^{T_{\alpha 2}}}, \tag{39a}$$

$$\pi_{Y_i} = \phi_2 \begin{cases} [\lambda_2(0)]^{T_{\beta 2}(i-1)/2} & : i \text{ is odd} \\ [\lambda_2(0)]^{T_{\beta 2}(i-2)/2} [\lambda_2(0)]^{T_{\text{on2}}-1} & : i \text{ is even} \end{cases}, i \in [1, 2M], \tag{39b}$$

$$\pi_{V_1} = \phi_2 [\lambda_2(0)]^{MT_{\beta 2}}, \quad \pi_{V_2} = \phi_2 [\lambda_2(0)]^{MT_{\beta 2}} \omega_3, \tag{39c}$$

$$\pi_{F_1} = \phi_2 \left(\frac{1}{[\lambda_2(0)]^{T_{\alpha 2}}} - 1 \right), \tag{39d}$$

$$\pi_{F_2} = \phi_2 \left(1 - [\lambda_2(0)]^{T_{\text{on2}}-1}\right) \left(1 + \frac{1-[\lambda_2(0)]^{MT_{\beta 2}}}{1-[\lambda_2(0)]^{T_{\beta 2}}} [\lambda_2(0)]^{T_{\beta 2}} \right), \tag{39e}$$

$$\pi_{F_3} = \phi_2 \left[1 - [\lambda_2(0)]^{MT_{\beta 2}}\right] \left[1 - \frac{1-[\lambda_2(0)]^{T_{\text{on2}}-1}}{1-[\lambda_2(0)]^{T_{\beta 2}}} \right], \tag{39f}$$

$$\pi_{F_i} = \phi_2 [\lambda_2(0)]^{MT_{\beta 2}} \sum_{\forall U \in V_2} \frac{\pi_U}{\pi_{V_1}} p_{U,F_i}, \quad i \in [4, 9]. \tag{39g}$$

All the expressions above depend on both the internal states of V_2 (Fig. 7) and their transition probabilities to the CRSs $F_i, i \in [4, 9]$. As such, we now analyze both of these factors.

3.3. Stationary probability – embedded Markov Chain – "deep sleep" internal states

In this section, we present the calculation of the stationary probabilities of the EMC corresponding to the SMC in Fig. 7. For the synchronization states, such probabilities follow these relationships:

$$\pi_{\hat{B}} = \pi_{V_1} p_{V_1,\hat{B}}, \quad \pi_{\hat{S}_i} = \pi_{V_1} p_{V_1,\hat{S}_i}, \; i \in [1, 2N], \tag{40a}$$

$$\pi_{\hat{G}_i} = \pi_{V_1} p_{V_1,\hat{G}_i}, \quad i \in [1, 2], \tag{40b}$$

$$\pi_{\hat{A}_i} = \pi_{V_1} p_{V_1,\hat{A}_i}, \quad i \in [1, 4]. \tag{40c}$$

For the non-synchronization states, such probabilities follow these relationships:

$$\pi_{\overline{S}_1} = \pi_{\overline{B}} p_{\overline{B},\overline{S}_1} + \pi_{\hat{B}} p_{\hat{B},\overline{S}_1}, \tag{41a}$$

$$\pi_{\overline{S}_i} = \pi_{\overline{S}_{i-1}} p_{\overline{S}_{i-1},\overline{S}_i} + \pi_{\hat{S}_{i-1}} p_{\hat{S}_{i-1},\overline{S}_i}, \quad i \in [2, 2N], \tag{41b}$$

$$\pi_{\overline{G}_1} = \pi_{\overline{S}_{2N}} p_{\overline{S}_{2N},\overline{G}_1} + \pi_{\overline{G}_2} p_{\overline{G}_2,\overline{G}_1} + \pi_{\hat{S}_{2N}} p_{\hat{S}_{2N},\overline{G}_1} + \pi_{\hat{G}_2} p_{\hat{G}_2,\overline{G}_1}, \tag{41c}$$

$$\pi_{\overline{G}_2} = \pi_{\overline{G}_1} p_{\overline{G}_1,\overline{G}_2} + \pi_{\hat{G}_1} p_{\hat{G}_1,\overline{G}_2}, \tag{41d}$$

$$\pi_{\overline{A}_1} = \pi_{\overline{B}} p_{\overline{B},\overline{A}_1} + \pi_{\hat{B}} p_{\hat{B},\overline{A}_1}, \tag{41e}$$

$$\pi_{\overline{A}_2} = \sum_{i=1}^{N} \pi_{\overline{S}_{2i-1}} p_{\overline{S}_{2i-1},\overline{A}_2} + \pi_{\overline{G}_1} p_{\overline{G}_1,\overline{A}_2} + \sum_{i=1}^{N} \pi_{\hat{S}_{2i-1}} p_{\hat{S}_{2i-1},\overline{A}_2} + \pi_{\hat{G}_1} p_{\hat{G}_1,\overline{A}_2}, \tag{41f}$$

$$\pi_{\overline{A}_3} = \pi_{\overline{G}_2} p_{\overline{G}_2,\overline{A}_3} + \pi_{\hat{G}_2} p_{\hat{G}_2,\overline{A}_3}, \tag{41g}$$

$$\pi_{\overline{A}_4} = \sum_{i=1}^{N} \pi_{\overline{S}_{2i}} p_{\overline{S}_{2i},\overline{A}_4} + \sum_{i=1}^{N} \pi_{\hat{S}_{2i}} p_{\hat{S}_{2i},\overline{A}_4}. \tag{41h}$$

For the exit states $C_i, i \in [0,5]$, such probabilities follow these relationships:

$$\pi_{C_0} = \pi_{V_1} p_{V_1,C_0}, \tag{42a}$$

$$\pi_{C_1} = \sum_{i=1}^{4} \pi_{\overline{A}_i} p_{\overline{A}_i,C_1} + \sum_{i=1}^{4} \pi_{\hat{A}_i} p_{\hat{A}_i,C_1} + \pi_{\overline{B}} p_{\overline{B},C_1} + \pi_{\hat{B}} p_{\hat{B},C_1} + \sum_{i=1}^{N} \pi_{\overline{S}_{2i-1}} p_{\overline{S}_{2i-1},C_1} + \sum_{i=1}^{N} \pi_{\hat{S}_{2i-1}} p_{\hat{S}_{2i-1},C_1} + \pi_{\overline{G}_1} p_{\overline{G}_1,C_1} + \pi_{\hat{G}_1} p_{\hat{G}_1,C_1}, \tag{42b}$$

$$\pi_{C_2} = \pi_{\hat{G}_2} p_{\hat{G}_2,C_2}, \quad \pi_{C_3} = \pi_{\overline{G}_2} p_{\overline{G}_2,C_3}, \tag{42c}$$

$$\pi_{C_4} = \sum_{i=1}^{N} \pi_{\hat{S}_{2i}} p_{\hat{S}_{2i},C_4}, \quad \pi_{C_5} = \sum_{i=1}^{N} \pi_{\overline{S}_{2i}} p_{\overline{S}_{2i},C_5}. \tag{42d}$$

Compared to the one of the EMC for the anchor CC and the SCell, the formulation of the internal states of the "deep sleep" cannot be expressed in a compact way similar to the one of Eq. (4) or Eq. (34). Nevertheless, it can be numerically solved in terms of π_{V_1} once the transition probabilities are known. Such transition probabilities depend on the BS packet arrival model, the probability distribution, and their service discipline not only at the SCell, but also at the anchor CC. To differentiate the parameters of the SCell from those of the anchor, we utilize the following notation for the latter: Λ_1 for the number of packets that arrive in a single subframe, $\lambda_1(k)$ for the PMF of Λ_1, λ_1 for the mean value of Λ_1, X_1 for the service time of a single packet, $b_1(l)$ for the PMF of X_1, and b_1 for the mean value of X_1. We now proceed to characterize the transition probabilities.

3.3.1. Transition probabilities to the synchronization states

The transition probabilities from V_1 to each of the synchronization states depend on the stationary probabilities of the EMC of the anchor CC and on whether a packet arrives at the BS for the SCell during the last subframe of V_1:

$$p_{V_1,C_0} = (1-\lambda_2(0)) \left(\tilde{\pi}_B + \tilde{\pi}_{G_1} + \sum_{i=1}^{N} \tilde{\pi}_{S_{2i-1}} + \sum_{i=1}^{4} \tilde{\pi}_{A_i} \right) \cdot [\lambda_2(0)]^{T_{\text{on2}}-1}, \tag{43a}$$

$$p_{V_1,\hat{B}} = [\lambda_2(0)]^{T_{\text{on2}}} \tilde{\pi}_B, \tag{43b}$$

$$p_{V_1,\hat{A}_i} = [\lambda_2(0)]^{T_{\text{on2}}} \tilde{\pi}_{A_i}, \quad i \in [1,4], \tag{43c}$$

$$p_{V_1,\hat{S}_{2i-1}} = [\lambda_2(0)]^{T_{\text{on2}}} \tilde{\pi}_{S_{2i-1}}, \quad i \in [1,N], \tag{43d}$$

$$p_{V_1,\hat{S}_{2i}} = [\lambda_2(0)]^{T_{\text{on2}}-1} \tilde{\pi}_{S_{2i}}, \quad i \in [1,N], \tag{43e}$$

$$p_{V_1,\hat{G}_1} = [\lambda_2(0)]^{T_{\text{on2}}} \tilde{\pi}_{G_1}, \quad p_{V_1,\hat{G}_2} = [\lambda_2(0)]^{T_{\text{on2}}-1} \tilde{\pi}_{G_2}, \tag{43f}$$

where for every state U, $\tilde{\pi}_U$ is obtained from Eq. (20). The transition probability p_{V_1,C_0} captures the event that no packet arrives for the SCell during the first $T_{\text{on1}}-1$ subframes of V_1, a packet arrives for the SCell during the last subframe, i.e., subframe T_{on1} of V_1, and the anchor CC is in a non-"sleep" state during subframe $T_{\text{on1}}+1$. When such event occurs, state C_0 is utilized to immediately notify the user of the need to transition the SCell out of the DSS.

The transition probabilities from the synchronization states to the rest of the states in Fig. 7 depend on the number of subframes left for the anchor to transition to its next state, which itself depends on the time instant when the SCell DRX lands in the synchronization state. These probabilities are now discussed.

3.3.2. Transition probabilities from the synchronization "on" states

The synchronization "on" states correspond to states $\hat{S}_{2i-1}, i \in [1,N]$, and $\hat{G}_1$. Consider an "on" state whose maximum length is ν subframes. Denote by P the subframe to be executed at the moment that the transition from V_1 takes place, i.e., there are up to $\nu-(P-1)$ subframes left until the end of the state. Then, given that $P=i, i \in [1,\nu]$,

$$\text{Prob}\{\Omega_1 \mid P=i,\nu\} = \sum_{j=1}^{\nu-(i-1)-1} q^{j-1} \lambda_2(0)[1-\lambda_1(0)] = \lambda_2(0)[1-\lambda_1(0)] \frac{1-q^{\nu-(i-1)-1}}{1-q}, \tag{44a}$$

$$\text{Prob}\{\Omega_2 \mid P=i,\nu\} = \sum_{j=1}^{\nu-(i-1)-1} q^{j-1} [1-\lambda_2(0)] = [1-\lambda_2(0)] \frac{1-q^{\nu-(i-1)-1}}{1-q}, \tag{44b}$$

$$\text{Prob}\{\Omega_3 \mid P=i,\nu\} = q^{\nu-(i-1)-1}, \tag{44c}$$

where $q=\lambda_1(0)\lambda_2(0)$. Ω_1, Ω_2, and Ω_3 indicate that the next transition is to a CRS of the anchor CC, to state C_1, and to the next "sleep" state of the anchor CC, respectively. In other words, they capture the required transition probabilities. The factor q^{j-1} is the probability that no packet arrives at the BS for the anchor CC or the SCell during $j-1$ subframes. To obtain the unconditional probabilities of Ω_1, Ω_2, and Ω_3, we need $\text{Prob}\{P=i\}$.

An "on" state can be seen as a group of substates of 1 subframe duration each. In the EMC of such group, the transition probability from every substate to the next one is the probability of no packet arriving in one subframe, i.e., $\lambda_1(0)$. Therefore, the stationary probability π_i of the i-th substate satisfies

$$\pi_i = \pi_{i-1}\lambda_1(0) = \pi_1 [\lambda_1(0)]^{i-1}. \tag{45}$$

The stationary probability $\tilde{\pi}_i$ of the i-th state in the SMC is

$$\tilde{\pi}_i = \frac{\pi_i H_i}{\sum_{\forall U'} \pi_{U'} H_{U'}} = \frac{\pi_i}{\sum_{\forall U'} \pi_{U'} H_{U'}} = \frac{\pi_1}{\sum_{\forall U'} \pi_{U'} H_{U'}} [\lambda_1(0)]^{i-1} = \tilde{\pi}_1 [\lambda_1(0)]^{i-1}. \tag{46}$$

Since the stationary probability $\tilde{\pi}_{\text{on}}$ of an "on" state, seen as a single state, in the SMC is equivalent to the sum of the stationary probability $\tilde{\pi}_i$ of its substates, it follows that

$$\tilde{\pi}_{\text{on}} = \sum_{i=1}^{\nu} \tilde{\pi}_i = \sum_{i=1}^{\nu} \tilde{\pi}_1 [\lambda_1(0)]^{i-1} = \tilde{\pi}_1 \frac{1-[\lambda_1(0)]^{\nu}}{1-[\lambda_1(0)]} = \frac{\tilde{\pi}_i}{[\lambda_1(0)]^{i-1}} \frac{1-[\lambda_1(0)]^{\nu}}{1-[\lambda_1(0)]}. \tag{47}$$

Therefore,

$$\tilde{\pi}_i = [\lambda_1(0)]^{i-1} \frac{1-[\lambda_1(0)]}{1-[\lambda_1(0)]^{\nu}} \tilde{\pi}_{\text{on}}, \tag{48}$$

from which we then obtain that

$$\text{Prob}\{P=i \mid \nu\} = [\lambda_1(0)]^{i-1} \frac{1-[\lambda_1(0)]}{1-[\lambda_1(0)]^{\nu}}. \tag{49}$$

We can now obtain the unconditional probabilities of Ω_1, Ω_2, and Ω_3 as

$$\mathrm{Prob}\{\Omega_j|\,v\} = \sum_{i=1}^{v} \mathrm{Prob}\{\Omega_j|\,P=i,v\}\mathrm{Prob}\{P=i|\,v\}, \quad i \in [1,3], \tag{50}$$

from which we then get

$$\mathrm{Prob}\{\Omega_1|\,v\} = \frac{\lambda_2(0)-q}{1-q}[1-f_1(v)], \tag{51a}$$

$$\mathrm{Prob}\{\Omega_2|\,v\} = \frac{1-\lambda_2(0)}{1-q}[1-f_1(v)], \tag{51b}$$

$$\mathrm{Prob}\{\Omega_3|\,v\} = f_1(v), \tag{51c}$$

where

$$f_1(x) = [\lambda_1(0)]^{x-1}\frac{1-\lambda_1(0)}{1-[\lambda_1(0)]^x}\frac{1-[\lambda_2(0)]^x}{1-\lambda_2(0)}, \tag{52}$$

and $q=\lambda_1(0)\lambda_2(0)$. Then, the transition probabilities from the "on" synchronization states of the SDCs are $p_{\hat{S}_{2i-1},\overline{A}_2} = \mathrm{Prob}\{\Omega_1|\,v=T_{\text{on}1}\}$, $p_{\hat{S}_{2i-1},C_1} = \mathrm{Prob}\{\Omega_2|\,v=T_{\text{on}1}\}$, and $p_{\hat{S}_{2i-1},\overline{S}_{2i}} = \mathrm{Prob}\{\Omega_3|\,v=T_{\text{on}1}\}$, $i\in[1,N]$. Similarly, the ones of the LDC are $p_{\hat{G}_1,\overline{A}_2} = \mathrm{Prob}\{\Omega_1|\,v=T_{\text{on}1}\}$, $p_{\hat{G}_1,C_1} = \mathrm{Prob}\{\Omega_2|\,v=T_{\text{on}1}\}$, and $p_{\hat{G}_1,\overline{G}_2} = \mathrm{Prob}\{\Omega_3|\,v=\ T_{\text{on}1}\}$, $i\in[1,N]$.

In addition to the transition probabilities, for $i\in[1,v]$, important relationships include

$$\mathrm{Prob}\{L=k|\,P=i,v\} = \begin{cases} q^{k-1}(1-q) & : 1 \le k < v-(i-1) \\ q^{k-1} & : k = v-(i-1) \end{cases}, \tag{53}$$

$$E\{L|\,P=i,v\} = \frac{1-q^{v-(i-1)}}{1-q}, \tag{54}$$

where L denotes the number of subframes spent in the "on" synchronization state. From the above, it follows that

$$E\{L|\,v\} = E\{E\{L|\,P=i,v\}\} = \frac{1-qf_1(v)}{1-q}. \tag{55}$$

Conceptually, $E\{L|\,v\}$ represents the holding time of an "on" synchronization state.

3.3.3. Transition probabilities from the synchronization inactivity period

State $\hat{B}$ represents the synchronization inactivity period. An inactivity period is very similar to an "on" state. The difference is that a transition to a CRS is possible from the last subframe of the inactivity period, and not of the "on" period. This difference impacts the formulation of the transition probabilities.

Consider that the inactivity period has a maximum length of v subframes. Denote by P the subframe to be executed at the moment that the transition from V_1 takes place, i.e., there are up to $v-(P-1)$ subframes left until the end of the state. Then, given that $P=i$, $i\in[1,v]$,

$$\mathrm{Prob}\{\Omega_1|\,P=i,v\} = \sum_{j=1}^{v-(i-1)} q^{j-1}\lambda_2(0)[1-\lambda_1(0)] = \lambda_2(0)[1-\lambda_1(0)]\frac{1-q^{v-(i-1)}}{1-q}, \tag{56a}$$

$$\mathrm{Prob}\{\Omega_2|\,P=i,v\} = \sum_{j=1}^{v-(i-1)} q^{j-1}[1-\lambda_2(0)] = [1-\lambda_2(0)]\frac{1-q^{v-(i-1)}}{1-q}, \tag{56b}$$

$$\mathrm{Prob}\{\Omega_3|\,P=i,v\} = q^{v-(i-1)}, \tag{56c}$$

where $q=\lambda_1(0)\lambda_2(0)$. Ω_1, Ω_2, and Ω_3 indicate that the next transition is to a CRS of the anchor CC, to C_1, and to the next "on" state of the anchor CC, respectively. In other words, they capture the required transition probabilities. The factor q^{j-1} is the probability that no packet arrives at the BS for the anchor CC or the SCell during $j-1$ subframes. To obtain the unconditional probabilities of Ω_1, Ω_2, and Ω_3, we need $\mathrm{Prob}\{P=i\}$. Such probability is found by following a similar analysis as the one for the synchronization "on" state, i.e., it follows Eqs. (49) and (50). Therefore, the unconditional probabilities of Ω_1, Ω_2, and Ω_3 become

$$\mathrm{Prob}\{\Omega_1|\,v\} = \frac{\lambda_2(0)-q}{1-q}[1-qf_1(v)], \tag{57a}$$

$$\mathrm{Prob}\{\Omega_2|\,v\} = \frac{1-\lambda_2(0)}{1-q}[1-qf_1(v)], \tag{57b}$$

$$\mathrm{Prob}\{\Omega_3|\,v\} = qf_1(v), \tag{57c}$$

where $f_1(x)$ is defined in Eq. (52). Then, the transition probabilities from the synchronization inactivity period are $p_{\hat{B},C_1} = \mathrm{Prob}\{\Omega_2|\,v=T_{\alpha 1}\}$, $p_{\hat{B},\overline{A}_1} = \mathrm{Prob}\{\Omega_1|\,v=T_{\alpha 1}\}$, and $p_{\hat{B},\overline{S}_1} = \mathrm{Prob}\{\Omega_3|\,v=\ T_{\alpha 1}\}$. By following a similar analysis as the one for the synchronization "on" state, the holding time of the synchronization inactivity period is found to follow Eq. (55).

3.3.4. Transition probabilities from the synchronization "sleep" states

The synchronization "sleep" states correspond to states $\hat{S}_{2i}$, $i\in[1,N]$ and $\hat{G}_2$. Consider a "sleep" state whose maximum length is v subframes. Denote by P the subframe to be executed at the moment that the transition from V_1 takes place, i.e., there are $v-(P-1)$ subframes left until the end of the state. Then, given that $P=i$, $i\in[1,v]$,

$$\mathrm{Prob}\{R=0|\,P=i,v\} = [\lambda_2(0)]^{v-(i-1)+1}, \tag{58a}$$

$$\begin{aligned}\mathrm{Prob}\{\Omega_1|\,P=i,v\} &= \left[1-[\lambda_1(0)]^v\right]\mathrm{Prob}\{R=0|\,P=i,v\} \\ &= \left[1-[\lambda_1(0)]^v\right][\lambda_2(0)]^{v-(i-1)+1},\end{aligned} \tag{58b}$$

$$\mathrm{Prob}\{\Omega_2|\,P=i,v\} = 1-\mathrm{Prob}\{R=0|\,P=i,v\} = 1-[\lambda_2(0)]^{v-(i-1)+1}, \tag{58c}$$

$$\begin{aligned}\mathrm{Prob}\{\Omega_3|\,P=i,v\} &= [\lambda_1(0)]^v\mathrm{Prob}\{R=0|\,P=i,v\} \\ &= [\lambda_1(0)]^v[\lambda_2(0)]^{v-(i-1)+1},\end{aligned} \tag{58d}$$

where R is the number of packets that arrive at the BS for the SCell by the end of the state. Ω_1, Ω_2, and Ω_3 indicate that the next transition is to a CRS of the anchor CC, to a state C_i, and to the next "on" state of the anchor CC, respectively. For a "sleep" state, P is a discrete and uniformly distributed random variable in the range $[1,v]$. It follows that

$$\begin{aligned}\mathrm{Prob}\{R=0|\,v\} &= \sum_{i=1}^{v}\mathrm{Prob}\{R=0|\,P=i,v\}\mathrm{Prob}\{P=i|\,v\} \\ &= \frac{[\lambda_2(0)]^2}{1-\lambda_2(0)}\frac{1-[\lambda_2(0)]^v}{v}.\end{aligned} \tag{59}$$

Let

$$f_2(x) = \frac{[\lambda_2(0)]^2}{1-\lambda_2(0)}\frac{1-[\lambda_2(0)]^x}{x}. \tag{60}$$

Then,

$$\mathrm{Prob}\{\Omega_1|\,v\} = \left[1-[\lambda_1(0)]^v\right]f_2(v), \tag{61a}$$

$$\mathrm{Prob}\{\Omega_2|\,v\} = 1-f_2(v), \tag{61b}$$

$$\mathrm{Prob}\{\Omega_3|\,v\} = [\lambda_1(0)]^v f_2(v). \tag{61c}$$

Therefore, the transition probabilities from the "sleep" periods are $p_{\hat{S}_{2i},C_4} = \text{Prob}\{\Omega_2 | v = T_{\beta 1} - T_{\text{on}1}\}$, $i \in [1, N]$; $p_{\hat{S}_{2i},\overline{S}_{2i+1}} = \text{Prob}\{\Omega_3 | v = T_{\beta 1} - T_{\text{on}1}\}$, $i \in [1, N-1]$; $p_{\hat{S}_{2N},\overline{G}_1} = \text{Prob}\{\Omega_3 | v = T_{\beta 1} - T_{\text{on}1}\}$; $p_{\hat{S}_{2i},\overline{A}_4} = \text{Prob}\{\Omega_1 | v = T_{\beta 1} - T_{\text{on}1}\}$, $i \in [1, N]$; $p_{\hat{G}_2,C_2} = \text{Prob}\{\Omega_2 | v = T_{\gamma 1} - T_{\text{on}1}\}$; $p_{\hat{G}_2,\overline{G}_1} = \text{Prob}\{\Omega_3 | v = T_{\gamma 1} - T_{\text{on}1}\}$; and $p_{\hat{G}_2,\overline{A}_3} = \text{Prob}\{\Omega_1 | v = T_{\gamma 1} - T_{\text{on}1}\}$. In addition to the transition probabilities, important relationships also include

$$E\{R | P = i, v\} = [v - (i-1) + 1]\lambda_2, \tag{62}$$

$$E\{R | v\} = E\{E\{R | P = i, v\}\} = \left[\frac{v+1}{2} + 1\right]\lambda_2, \tag{63}$$

$$\text{Prob}\{L = i | v\} = \text{Prob}\{P = v - (i-1) | v\} = \frac{1}{v}, \quad i \in [1, v], \tag{64}$$

where L denotes the number of subframes left to be executed until the end of the "sleep" state. Since L is also uniformly distributed over $[1, v]$, we have that

$$E\{L | v\} = \frac{v+1}{2}. \tag{65}$$

Let $\check{R}$ denote R conditioned on being greater than zero, i.e., $\check{R}$ is the number of packets in the BS for the SCell given that at least one such packet arrived. Then,

$$\text{Prob}\{\check{R} = k | v\} = \begin{cases} \dfrac{\text{Prob}\{R = k | v\}}{1 - \text{Prob}\{R = 0 | v\}} & : k > 0 \\ 0 & : k = 0 \end{cases}, \tag{66}$$

$$E\{\check{R} | v\} = \frac{E\{R | v\}}{1 - \text{Prob}\{R = 0 | v\}} = \frac{1 + \frac{v+1}{2}}{1 - f_2(v)}\lambda_2. \tag{67}$$

Conceptually, $\check{R}$ represents the number of buffered packets for the SCell if the BS determines that it should trigger the activation of the SCell at the end of a "sleep" synchronization state, and $E\{L | v\}$ represents the holding time of a "sleep" synchronization state.

3.3.5. Transition probabilities from the synchronization continuous reception states

Compared to the previously described synchronization states, a synchronization CRS does not have a maximum duration that applies to every instance of such state.

Let P_- be a random variable corresponding to the number of subframes left until the end of the synchronization CRS at the moment that the transition from V_1 takes place, i.e., if the UE were not tracking such state for the presence of a PDCCH for the SCell, such state would have been executed for P_- more subframes. Then, it follows that

$$\text{Prob}\{\Omega_2 | P_- = m\} = 1 - [\lambda_2(0)]^m, \tag{68a}$$

$$\text{Prob}\{\Omega_3 | P_- = m\} = [\lambda_2(0)]^m, \tag{68b}$$

where Ω_2 and Ω_3 indicate that the next transition is to C_1, and to the next inactivity period, respectively. To obtain the unconditional probabilities of Ω_2 and Ω_3, we need $\text{Prob}\{P_- = m\}$. In contrast to the transition probabilities discussed in the previous section, there is no explicit formulation for $\text{Prob}\{P_- = m\}$; nevertheless, we can obtain one for its probability-generating function (PGF). Such approach is useful because

$$\text{Prob}\{\Omega_2\} = \sum_{i=1}^{\infty} \text{Prob}\{\Omega_2 | P_- = m\}\text{Prob}\{P_- = m\} = 1 - \mathcal{Z}_{P_-}(z)\big|_{z=\lambda_2(0)}, \tag{69a}$$

$$\text{Prob}\{\Omega_3\} = \sum_{i=1}^{\infty} \text{Prob}\{\Omega_3 | P_- = m\}\text{Prob}\{P_- = m\} = \mathcal{Z}_{P_-}(z)\big|_{z=\lambda_2(0)}, \tag{69b}$$

where

$$\mathcal{Z}_{P_-}(z) = \sum_{m=1}^{\infty} z^m \text{Prob}\{P_- = m\}, \tag{70}$$

i.e., $\mathcal{Z}_{P_-}(z)$ represents the PGF of P_-. We now describe how to obtain an expression for such PGF.

Let P be a random variable corresponding to the number of subframes of the CRS of interest. Let P_+ be a random variable corresponding to the number of subframes of the CRS landed after transitioning from V_1. An instance of a CRS lasting j subframes has a chance of including the landing subframe with a probability proportional to j. Therefore, the probability that P_+ has j subframes is given by

$$\text{Prob}\{P_+ = j\} = \frac{j\text{Prob}\{P = j\}}{E\{P\}}. \tag{71}$$

The position of the landed subframe within the synchronization CRS is uniformly distributed over the length of the state. Hence, the probability that there are k remaining subframes in the synchronization CRS is

$$\text{Prob}\{P_- = k | P_+ = j\} = \frac{1}{j}, \quad j \geq 1, \quad k = 1, 2, \ldots, j. \tag{72}$$

So,

$$\text{Prob}\{P_- = k\} = \sum_{j=1}^{\infty} \text{Prob}\{P_- = k | P_+ = j\}\text{Prob}\{P_+ = j\} = \frac{\text{Prob}\{P \geq k\}}{E\{P\}}, \tag{73}$$

then, the PGF of P_- becomes

$$\mathcal{Z}_{P_-}(z) = \frac{z}{1-z}\frac{1 - \mathcal{Z}_P(z)}{E\{P\}}, \tag{74}$$

where $\mathcal{Z}_P(z)$ is the PGF of P, i.e., the PGF of the length (in subframes) of a CRS. If such state started with $\check{R}$ subframes, then

$$P = \sum_{i=1}^{\check{R}} P_*, \tag{75}$$

where P_* is a random variable corresponding to the length of a CRS caused by one packet in the buffer, i.e., the length of a busy period caused by one packet, in queuing theory terminology. Therefore, the PGF of P becomes

$$\mathcal{Z}_P(z) = \mathcal{Z}_{\check{R}}(\mathcal{Z}_{P_*}(z)), \tag{76}$$

where $\mathcal{Z}_{\check{R}}(z)$ is the PGF of $\check{R}$. Since the PMF of $\check{R}(z)$ follows Eq. (66), its PGF is

$$\mathcal{Z}_{\check{R}}(z) = \frac{\mathcal{Z}_R(z) - \text{Prob}\{R = 0\}}{1 - \text{Prob}\{R = 0\}}, \tag{77}$$

where R is the number of packets buffered during the state that preceded the CRS. If such state buffered packets during ν subframes, then we would have that $\text{Prob}\{R = 0\} = [\lambda_1(0)]^\nu$ and $\mathcal{Z}_R(z) = [\mathcal{Z}_{A_1}(z)]^\nu$. Therefore, plugging into Eq. (77) and then into Eq. (76), we get

$$\mathcal{Z}_P(z) = \frac{[\mathcal{Z}_{A_1}(\mathcal{Z}_{P_*}(z))]^\nu - [\lambda_1(0)]^\nu}{1 - [\lambda_1(0)]^\nu}. \tag{78}$$

The expected value of P can be found from

$$E\{P\} = \frac{d}{dz}\mathcal{Z}_P(z)\bigg|_{z=1} = \frac{\nu\lambda_1}{1 - [\lambda_1(0)]^\nu}E\{P_*\}, \tag{79}$$

where $E\{P_*\}$ is obtained from Eq. (14) by considering that the initial number of packets in the buffer is 1, i.e.,

$$E\{P_*\} = \frac{b_1}{1 - \rho_1}, \tag{80}$$

where $\rho_1 = \lambda_1 b_1$. Therefore, by plugging Eq. (80) into Eq. (79), we have

$$E\{P\} = \frac{\rho_1}{1-\rho_1}\frac{v}{1-[\lambda_1(0)]^v}. \tag{81}$$

By plugging Eqs. (78) and (81) into Eq. (74), we obtain

$$\mathcal{Z}_{P_-}(z) = \frac{z}{1-z}\frac{1-\rho_1}{\rho_1}\frac{1-\left[\mathcal{Z}_{\Lambda_1}\left(\mathcal{Z}_{P_*}(z)\right)\right]^v}{v}. \tag{82}$$

From Eqs. (69a) and (69b), we can now obtain the probabilities of Ω_1 and Ω_2:

$$\text{Prob}\{\Omega_2\} = 1 - f_3(v), \tag{83a}$$

$$\text{Prob}\{\Omega_3\} = f_3(v), \tag{83b}$$

where

$$f_3(x) = \frac{1-\rho_1}{\rho_1}\frac{\lambda_2(0)}{1-\lambda_2(0)}\left.\frac{1-\left[\mathcal{Z}_{\Lambda_1}\left(\mathcal{Z}_{P_*}(z)\right)\right]^x}{x}\right|_{z=\lambda_2(0)}, \tag{84}$$

and $\mathcal{Z}_{P_*}(z)$ is obtained from Takagi (1993) as the PGF of the length of a busy period triggered by the arrival of one packet:

$$\mathcal{Z}_{P_*}(u) = \sum_{n=1}^{\infty}\frac{u^n}{n!}\frac{d^{n-1}}{dz^{n-1}}\left.\left\{\left[\frac{d}{dz}\mathcal{Z}_{X_1}(z)\right]\left[\mathcal{Z}_{\Lambda_1}\left(\mathcal{Z}_{X_1}(z)\right)\right]^n\right\}\right|_{z=0}. \tag{85}$$

Then, the transition probabilities from the continuous reception periods can be obtained as follows: $p_{\hat{A}_1,\overline{B}} = p_{\hat{A}_2,\overline{B}} = f_3(1)$, $p_{\hat{A}_1,C_1} = p_{\hat{A}_2,C_1} = 1 - f_3(1)$, $p_{\hat{A}_4,\overline{B}} = f_3(T_{\beta 1} - T_{\text{on}1} + 1)$, $p_{\hat{A}_4,C_1} = 1 - f_3(T_{\beta 1} - T_{\text{on}1} + 1)$, $p_{\hat{A}_3,\overline{B}} = f_3(T_{\gamma 1} - T_{\text{on}1} + 1)$, and $p_{\hat{A}_3,C_1} = 1 - f_3(T_{\gamma 1} - T_{\text{on}1} + 1)$. In addition to the transition probabilities, important relationships include

$$\text{Prob}\{L = k \mid P_- = m\} = \begin{cases} [\lambda_2(0)]^{k-1}[1-\lambda_2(0)] & : 1 \le k < m \\ [\lambda_2(0)]^{k-1} & : k = m \end{cases} \tag{86}$$

$$E\{L \mid P_- = m\} = \frac{1-[\lambda_2(0)]^m}{1-\lambda_2(0)}, \tag{87}$$

where L denotes the number of subframes spent in the synchronization CRS. From the above, it follows that

$$E\{L\} = E\{E\{L \mid P_- = m\}\} = \frac{1-f_3(v)}{1-\lambda_2(0)}. \tag{88}$$

Conceptually, $E\{L\}$ represents the holding time of a synchronization CRS.

3.3.6. Transition probabilities for non-synchronization states

For the non-synchronization states, we use most of the expressions previously developed for the synchronization states. We can do so because a non-synchronization state is equivalent to a synchronization state that always starts at subframe 1 of the original state. Particularly, for the "on," inactivity, and "sleep" states, we only need to set $P=1$ in Eq. (44), Eq. (56), Eq. (58), respectively. Then, we obtain

$$p_{\overline{B},\overline{S}_1} = q^{T_{\alpha 1}}, \tag{89a}$$

$$p_{\overline{B},\overline{A}_1} = [\lambda_2(0) - q]\frac{1-q^{T_{\alpha 1}}}{1-q}, \tag{89b}$$

$$p_{\overline{B},C_1} = [1-\lambda_2(0)]\frac{1-q^{T_{\alpha 1}}}{1-q}, \tag{89c}$$

$$p_{\overline{S}_{2i-1},\overline{S}_{2i}} = q^{T_{\text{on}1}-1}, \quad i \in [1, N], \tag{89d}$$

$$p_{\overline{S}_{2i-1},\overline{A}_2} = [\lambda_2(0) - q]\frac{1-q^{T_{\text{on}1}-1}}{1-q}, \quad i \in [1, N], \tag{89e}$$

$$p_{\overline{S}_{2i-1},C_1} = [1-\lambda_2(0)]\frac{1-q^{T_{\text{on}1}-1}}{1-q}, \quad i \in [1, N], \tag{89f}$$

$$p_{\overline{S}_{2N},\overline{G}_1} = q^{T_{\beta 1}-T_{\text{on}1}+1}, \tag{89g}$$

$$p_{\overline{S}_{2i},\overline{S}_{2i+1}} = q^{T_{\beta 1}-T_{\text{on}1}+1}, \quad i \in [1, N-1], \tag{89h}$$

$$p_{\overline{S}_{2i},\overline{A}_4} = [\lambda_2(0)]^{T_{\beta 1}-T_{\text{on}1}+1} - q^{T_{\beta 1}-T_{\text{on}1}+1}, \quad i \in [1, N], \tag{89i}$$

$$p_{\overline{S}_{2i},C_5} = 1 - [\lambda_2(0)]^{T_{\beta 1}-T_{\text{on}1}+1}, \quad i \in [1, N], \tag{89j}$$

$$p_{\overline{G}_2,\overline{G}_1} = q^{T_{\gamma 1}-T_{\text{on}1}+1}, \tag{89k}$$

$$p_{\overline{G}_2,\overline{A}_3} = [\lambda_2(0)]^{T_{\gamma 1}-T_{\text{on}1}+1} - q^{T_{\gamma 1}-T_{\text{on}1}+1}, \tag{89l}$$

$$p_{\overline{G}_2,C_3} = 1 - [\lambda_2(0)]^{T_{\gamma 1}-T_{\text{on}1}+1}. \tag{89m}$$

For the CRSs, we use the expressions in Eq. (69) and replace the PGF of P_- with the PGF of P (Eq. (78)), leading to $p_{\overline{A}_1,C_1} = p_{\overline{A}_2,C_1} = f_4(1)$, $p_{\overline{A}_1,\overline{B}} = p_{\overline{A}_2,\overline{B}} = 1 - f_4(1)$, $p_{\overline{A}_3,C_1} = f_4(T_{\gamma 1} - T_{\text{on}1} + 1)$, $p_{\overline{A}_3,\overline{B}} = 1 - f_4(T_{\gamma 1} - T_{\text{on}1} + 1)$, $p_{\overline{A}_4,C_1} = f_4(T_{\beta 1} - T_{\text{on}1} + 1)$, and $p_{\overline{A}_4,\overline{B}} = 1 - f_4(T_{\beta 1} - T_{\text{on}1} + 1)$, where

$$f_4(x) = \left.\frac{1-\left[\mathcal{Z}_{\Lambda_1}\left(\mathcal{Z}_{P_*}(z)\right)\right]^x}{1-[\lambda_1(0)]^x}\right|_{z=\lambda_2(0)}. \tag{90}$$

3.3.7. Transition probabilities for exit states

States $C_i, i \in [0, 5]$, correspond to the exit states, i.e., the states that represent the exit from the DSS. Their transition probabilities are

$$p_{C_i,F_{i+4}} = 1, \quad i \in [0, 5]. \tag{91}$$

At this point, all the transition probabilities have been defined, and the stationary probabilities of the EMC can be evaluated. In addition to the stationary probabilities of the EMC, the holding time of each state is required to compute the performance metrics.

3.4. Holding time

3.4.1. "Deep sleep" internal states

For the synchronization states inside the DSS, the holding time was discussed jointly with their transition probabilities in Sections 3.3.2–3.3.4. Here we summarize the expressions for those holding times H:

$$H_{\hat{S}_{2i}} = \frac{T_{\beta 1} - T_{\text{on}1} + 1}{2}, \quad i \in [1, N], \tag{92a}$$

$$H_{\hat{S}_{2i-1}} = \frac{1 - qf_1(T_{\text{on}1})}{1-q}, \quad i \in [1, N], \tag{92b}$$

$$H_{\hat{G}_1} = \frac{1 - qf_1(T_{\text{on}1})}{1-q}, \quad H_{\hat{G}_2} = \frac{T_{\gamma 1} - T_{\text{on}1} + 1}{2}, \tag{92c}$$

$$H_{\hat{B}} = \frac{1 - qf_1(T_{\alpha 1})}{1-q}, \quad H_{\hat{A}_1} = H_{\hat{A}_2} = \frac{1 - f_3(1)}{1-\lambda_2(0)}, \tag{92d}$$

$$H_{\hat{A}_3} = \frac{1 - f_3(T_{\gamma 1} - T_{\text{on}1} + 1)}{1-\lambda_2(0)}, \tag{92e}$$

$$H_{\hat{A}_4} = \frac{1-f_3(T_{\beta 1}-T_{\text{on}1}+1)}{1-\lambda_2(0)}, \tag{92f}$$

where $f_1(x)$ is defined in Eq. (52), and $f_3(x)$ is defined in Eq. (84).

For the non-synchronization states inside the DSS, the holding time is obtained following a similar approach as the one for the transition probabilities in Section 3.3.6. Particularly, for the "on" and inactivity states, we only need to set $P=1$ in Eq. (54). For the "sleep" and exit states $C_i, i \in [0,5]$, the holding time is a deterministic value:

$$H_{\overline{S}_{2i}} = T_{\beta 1}-T_{\text{on}1}, \quad i \in [1,N], \tag{93a}$$

$$H_{\overline{S}_{2i-1}} = \frac{1-q^{T_{\text{on}1}}}{1-q}, \quad i \in [1,N], \tag{93b}$$

$$H_{\overline{B}} = \frac{1-q^{T_{\alpha 1}}}{1-q}, \quad H_{\overline{G}_1} = \frac{1-q^{T_{\text{on}1}}}{1-q}, \tag{93c}$$

$$H_{\overline{G}_2} = T_{\gamma 1}-T_{\text{on}1}, \quad H_{C_i}=1, \; i \in [0,5]. \tag{93d}$$

For the non-synchronization CRSs inside the DSS, we use the expression in Eq. (87) and replace the PGF of P_- with the PGF of P (Eq. (78)) when calculating the holding time, leading to

$$H_{\overline{A}_1} = H_{\overline{A}_2} = \frac{f_4(1)}{1-\lambda_2(0)}, \tag{94a}$$

$$H_{\overline{A}_3} = \frac{f_4(T_{\gamma 1}-T_{\text{on}1}+1)}{1-\lambda_2(0)}, \tag{94b}$$

$$H_{\overline{A}_4} = \frac{f_4\left(T_{\beta 1}-T_{\text{on}1}+1\right)}{1-\lambda_2(0)}, \tag{94c}$$

where $f_4(x)$ is defined in Eq. (90).

3.4.2. SCell

For the holding time of the SCell states (Fig. 5), we can directly apply the expressions developed in Section 2.3 by adjusting for the parameters of the SCell:

$$H_R = \frac{1-[\lambda_2(0)]^{T_{\alpha 2}}}{1-\lambda_2(0)}, \tag{95a}$$

$$H_{Y_{2i-1}} = \frac{1-[\lambda_2(0)]^{T_{\text{on}2}}}{1-\lambda_2(0)}, \quad i \in [1,N], \tag{95b}$$

$$H_{Y_{2i}} = T_{\beta 2}-T_{\text{on}2}, \quad i \in [1,N], \tag{95c}$$

$$H_{V_1} = \frac{1-[\lambda_2(0)]^{T_{\text{on}2}}}{1-\lambda_2(0)}, \tag{95d}$$

$$H_{F_1} = H_{F_2} = \frac{\rho_2}{1-\rho_2}\frac{1}{1-\lambda_2(0)}, \tag{95e}$$

$$H_{F_3} = \frac{\rho_2}{1-\rho_2}\frac{T_{\beta 2}-T_{\text{on}2}+1}{1-[\lambda_2(0)]^{T_{\beta 2}-T_{\text{on}2}+1}}. \tag{95f}$$

The previous expressions account for the inactivity period, SDCs, state V_1, and CRSs $F_i, i \in [1,3]$. The last three states are related to the arrival of packets outside the "deep sleep". On the other hand, states $F_i, i \in [4,9]$, are related to the arrival of packets within the "deep sleep," and their holding times are now analyzed.

From Eq. (15), we have that the holding time of a CRS depends on the expected value of the number of packets in the BS buffer at the moment that the state starts. For states $F_i, i \in [4,9]$, such expected value $E\{R_{F_i}\}$ is the sum of

- the expected value of the number of packets received during C_{i-4}, i.e., λ_2 packets, and
- the expected value $E\{R_{C_{i-4}}\}$ of the number of packets in the BS buffer when C_{i-4} started,

$$\begin{aligned}\Psi_2 = {} & \left[1-[\lambda_2(0)]^{T_{\text{on}2}-1}\right][\lambda_2(0)]^{MT_{\beta 2}}H_{F_2} + \left[1-[\lambda_2(0)]^{MT_{\beta 2}}\right]H_{F_3} \\ & + [\lambda_2(0)]^{MT_{\beta 2}}\left[H_{Y_1} + \sum_{i=4}^{9}\frac{\pi_{C_{i-4}}}{\pi_{V_1}}H_{F_i} + \sum_{\forall U \in V_2}\frac{\pi_U}{\pi_{V_1}}H_U\right] \\ & + \frac{1-[\lambda_2(0)]^{MT_{\beta 2}}}{1-[\lambda_2(0)]^{T_{\beta 2}}}\left[H_{Y_1} + [\lambda_2(0)]^{T_{\text{on}2}-1}H_{Y_2}\right. \\ & \left. + \left[1-[\lambda_2(0)]^{T_{\text{on}2}-1}\right][H_{F_2}-H_{F_3}]\right] + \frac{H_R + \left(1-[\lambda_2(0)]^{T_{\alpha 2}}\right)H_{F_1}}{[\lambda_2(0)]^{T_{\alpha 2}}}.\end{aligned} \tag{96}$$

i.e.,

$$E\{R_{F_i}\} = \lambda_2 + E\{R_{C_{i-4}}\} \quad i \in [4,9]. \tag{97}$$

Then, applying Eq. (15), we have that

$$H_{F_i} = E\{R_{F_i}\}\frac{b_2}{1-\rho_2} = \frac{\rho_2}{1-\rho_2}\left[1+\frac{E\{R_{C_{i-4}}\}}{\lambda_2}\right], \quad i \in [4,9]. \tag{98}$$

$E\{R_{C_{i-4}}\}$ can be computed from Eq. (18) for $i \in \{4,5,7,9\}$, i.e., for the states C_i that are reached from any state except the synchronization "sleep" states. The reason is that the buffering time that precedes states $C_i, i \in \{0,1,3,5\}$, is a deterministic value. So,

$$E\{R_{C_0}\} = E\{R_{C_1}\} = \lambda_2\frac{1}{1-\lambda_2(0)}, \tag{99a}$$

$$E\{R_{C_3}\} = \lambda_2\frac{T_{\gamma 1}-T_{\text{on}1}+1}{1-[\lambda_2(0)]^{T_{\gamma 1}-T_{\text{on}1}+1}}, \tag{99b}$$

$$E\{R_{C_5}\} = \lambda_2\frac{T_{\beta 1}-T_{\text{on}1}+1}{1-[\lambda_2(0)]^{T_{\beta 1}-T_{\text{on}1}+1}}. \tag{99c}$$

For $i \in \{2,4\}$, $E\{R_{C_i}\}$ is determined by Eq. (67), i.e., by the expected number of packets at the end of the preceding "sleep" state, given that at least one such packet arrived. So,

$$E\{R_{C_2}\} = \lambda_2 f_5(T_{\gamma 1}-T_{\text{on}1}), \tag{100a}$$

$$E\{R_{C_4}\} = \lambda_2 f_5\left(T_{\beta 1}-T_{\text{on}1}\right), \tag{100b}$$

where

$$f_5(x) = \frac{1+\frac{x+1}{2}}{1-f_2(x)}, \tag{101}$$

and $f_2(x)$ is defined in Eq. (60). Having $E\{R_{C_i}\}, i \in [0,5]$, we can plug it into Eq. (98) and find the remaining holding times:

$$H_{F_4} = H_{F_5} = \frac{\rho_2}{1-\rho_2}\left[1+\frac{1}{1-\lambda_2(0)}\right], \tag{102a}$$

$$H_{F_6} = \frac{\rho_2}{1-\rho_2}[1+f_5(T_{\gamma 1}-T_{\text{on}1})], \tag{102b}$$

$$H_{F_7} = \frac{\rho_2}{1-\rho_2}\left[1+\frac{T_{\gamma 1}-T_{\text{on}1}+1}{1-[\lambda_2(0)]^{T_{\gamma 1}-T_{\text{on}1}+1}}\right], \tag{102c}$$

$$H_{F_8} = \frac{\rho_2}{1-\rho_2}\left[1+f_5\left(T_{\beta 1}-T_{\text{on}1}\right)\right], \tag{102d}$$

$$H_{F_9} = \frac{\rho_2}{1-\rho_2}\left[1+\frac{T_{\beta 1}-T_{\text{on}1}+1}{1-[\lambda_2(0)]^{T_{\beta 1}-T_{\text{on}1}+1}}\right]. \tag{102e}$$

3.5. Performance metrics

The main performance metrics associated with any DRX scheme are the amount of energy saved and the packet delay, also known as waiting time in queuing theory terminology. Since the metrics for the anchor CC correspond to the ones already analyzed and evaluated in Section 2, here we focus on evaluating the performance metrics for the SCell.

3.5.1. Energy savings

As described in Section 2.4.1, the amount of energy saved is defined as the total amount of time spent in the "sleep" and DSS. This value is obtained from the stationary probabilities of the SMC, which we derive from the stationary probabilities of the EMC in Eqs. (39)–(42), obtained in Sections 3.2 and 3.3.

For any state U, its stationary probability $\tilde{\pi}_U$ in the SMC is defined by Eq. (20). Then, the energy savings $\tau_{\beta2}$ and τ_{ds} provided by the SDCs and the DSS, respectively, are

$$\tau_{\beta2} = \sum_{i=1}^{M} \tilde{\pi}_{Y_{2i}}, \quad \tau_{\mathrm{ds}} = \sum_{\forall U \in V_2}^{M} \tilde{\pi}_U. \tag{103}$$

Replacing the expressions for the stationary probabilities of the SMC, $\tau_{\beta2}$ and τ_{ds} become

$$\tau_{\beta2} = \frac{T_{\beta2} - T_{\mathrm{on2}}}{\Psi_2} \frac{1 - [\lambda_2(0)]^{MT_{\beta2}}}{1 - [\lambda_2(0)]^{T_{\beta2}}} [\lambda_2(0)]^{T_{\mathrm{on2}}-1}, \tag{104a}$$

$$\tau_{\mathrm{ds}} = \frac{[\lambda_2(0)]^{MT_{\beta2}}}{\Psi_2} \sum_{U \in V_2} \frac{\pi_U}{\pi_{V_1}} H_U, \tag{104b}$$

where Ψ_2 is described by Eq. (96). Then, the total energy savings τ_2 become

$$\tau_2 = \tau_{\beta2} + \tau_{\mathrm{ds}}. \tag{105}$$

If in a given implementation the power consumption during the "non-sleep", "sleep", and DSS states are, respectively, $P_{\max}$, $c_0 P_{\max}$ $(0 \le c_0 \le 1)$, and $c_1 P_{\max}$ $(0 \le c_1 \le 1)$, then the implementation-dependent energy savings are

$$(1 - c_0)\tau_{\beta2} + (1 - c_1)\tau_{\mathrm{ds}}. \tag{106}$$

In general, it can be assumed that $c_1 \ge c_0$, i.e., the amount of power consumed during the DSS is no less than the one consumed during the regular "sleep" periods. From Eqs. (24) and (106), we have that in order for the implementation-dependent energy savings of the cross-carrier-aware DRX to be greater than those of the classical DRX, the following condition must be satisfied:

$$(1 - c_1) \ge \frac{\tau - \tau_{\beta2}}{\tau_{\mathrm{ds}}}(1 - c_0). \tag{107}$$

$$\begin{aligned} E\{\Gamma_2\} = \frac{1}{\sum_{j=1}^{9} \pi_{F_j} H_{F_j}} \Bigg[\frac{1}{2} \Big[\left(T_{\beta2} - T_{\mathrm{on2}}\right) \pi_{F_3} H_{F_3} + \pi_{F_4} H_{F_4} + \pi_{F_5} H_{F_5} \\ + (T_{\gamma1} - T_{\mathrm{on1}} + 1) \pi_{F_7} H_{F_7} + \left(T_{\beta1} - T_{\mathrm{on1}} + 1\right) \pi_{F_9} H_{F_9} \Big]. \\ + \frac{1}{3} \Bigg[\frac{(T_{\gamma1} - T_{\mathrm{on1}})^2 + 6(T_{\gamma1} - T_{\mathrm{on1}}) + 11}{(T_{\gamma1} - T_{\mathrm{on1}}) + 5} \pi_{F_6} H_{F_6} \\ + \frac{\left(T_{\beta1} - T_{\mathrm{on1}}\right)^2 + 6\left(T_{\beta1} - T_{\mathrm{on1}}\right) + 11}{\left(T_{\beta1} - T_{\mathrm{on1}}\right) + 5} \pi_{F_8} H_{F_8} \Bigg] \Bigg] + E\{\Upsilon_1\}. \end{aligned} \tag{108}$$

For $\tau_{\beta2} \ge \tau$ the above condition is always satisfied. In the ideal case where $c_1 = c_0$, the above condition becomes $\tau_2 = \tau_{\mathrm{ds}} + \tau_{\beta2} > = \tau$, i.e., a comparison between the implementation-independent metrics for energy savings.

3.5.2. Delay

To calculate the expected value $E\{\Gamma_2\}$ of the packet delay in the SCell, we need to compute (a) the expected value of the delay Υ_i experienced by the packets sent in $F_i, i \in [1, 9]$, and (b) the probability of a packet to be sent in each of such states. As discussed in Section 2.4.2, we apply the results from queuing theory that establish the expected value $E\{\Upsilon\}$ of the packet waiting time in a system with vacation (Takagi, 1993). In such context,

$$E\{\Upsilon | v\} = \frac{[\lambda_2]^2 E\{[X_2]^2\} + b_2 E\{[\Lambda_2]^2\} - \rho_2(\lambda_2 + 1)}{2\lambda_2(1 - \rho_2)} + \frac{E\{v(v-1)\}}{2E\{v\}}, \tag{109}$$

where v is the length of the vacation, the first term represents the waiting time in a system without vacation, and the second term represents the residual life of the vacation time. In the context of DRX, v corresponds to the amount of time the BS buffers packets before entering a CRS. Therefore, v is a deterministic value equal to 1 for F_1 and F_2 and $T_{\beta2} - T_{\mathrm{on2}} + 1$ for F_3. For $F_i, i \in [4, 9]$, v is the sum of the amount spent in state C_{i-4}, i.e., 1 subframe, and the amount of buffering time preceding that state. In particular, v is a deterministic value equal to 2 for F_4 and F_5, $T_{\gamma1} + T_{\mathrm{on1}} + 2$ for F_7, and $T_{\beta1} - T_{\mathrm{on1}} + 2$ for F_9. On the other hand, v is a discrete uniformly distributed random variable in the range $[3, T_{\gamma1} - T_{\mathrm{on1}} + 2]$ for F_6 and in the range $[3, T_{\beta1} - T_{\mathrm{on1}} + 2]$ for F_8. It then follows that

$$E\{\Upsilon_1\} = E\{\Upsilon_2\} = \frac{[\lambda_2]^2 E\{[X_2]^2\} + b_2 E\{[\Lambda_2]^2\} - \rho_2(\lambda_2 + 1)}{2\lambda_2(1 - \rho_2)}, \tag{110a}$$

$$E\{\Upsilon_3\} = E\{\Upsilon_1\} + \frac{T_{\beta2} - T_{\mathrm{on2}}}{2}, \tag{110b}$$

$$E\{\Upsilon_4\} = E\{\Upsilon_5\} = E\{\Upsilon_1\} + \tfrac{1}{2}, \tag{110c}$$

$$E\{\Upsilon_6\} = E\{\Upsilon_1\} + \frac{1}{3} \frac{(T_{\gamma1} - T_{\mathrm{on1}})^2 + 6(T_{\gamma1} - T_{\mathrm{on1}}) + 11}{(T_{\gamma1} - T_{\mathrm{on1}}) + 5}, \tag{110d}$$

$$E\{\Upsilon_7\} = E\{\Upsilon_1\} + \frac{T_{\gamma1} + T_{\mathrm{on1}} + 1}{2}, \tag{110e}$$

$$E\{\Upsilon_8\} = E\{\Upsilon_1\} + \frac{1}{3} \frac{\left(T_{\beta1} - T_{\mathrm{on1}}\right)^2 + 6\left(T_{\beta1} - T_{\mathrm{on1}}\right) + 11}{\left(T_{\beta1} - T_{\mathrm{on1}}\right) + 5}, \tag{110f}$$

$$E\{\Upsilon_9\} = E\{\Upsilon_1\} + \frac{T_{\beta1} + T_{\mathrm{on1}} + 1}{2}. \tag{110g}$$

We now compute the probability of a packet being sent from state F_i. From Eq. (28), we have that such probability is

$$\mathrm{Prob}\{\Phi = F_i\} = \frac{\pi_{F_i} H_{F_i}}{\sum_{j=1}^{9} \pi_{F_j} H_{F_j}}, \tag{111}$$

where Φ denotes the state from which the packet is sent. We now see that

$$\begin{aligned} E\{\Gamma_2\} = E\{E\{\Gamma_2 | \Phi\}\} = \sum_{i=1}^{9} E\{\Gamma_2 | \Phi = F_i\} \mathrm{Prob}\{\Phi = F_i\} \\ = \sum_{i=1}^{9} E\{\Upsilon_i\} \mathrm{Prob}\{\Phi = F_i\}. \end{aligned} \tag{112}$$

After further simplification, this expression becomes Eq. (108). As mentioned previously, the second term represents the waiting time in a system with no DRX. Thus, the first term denotes the additional waiting time due to the cross-carrier-aware DRX.

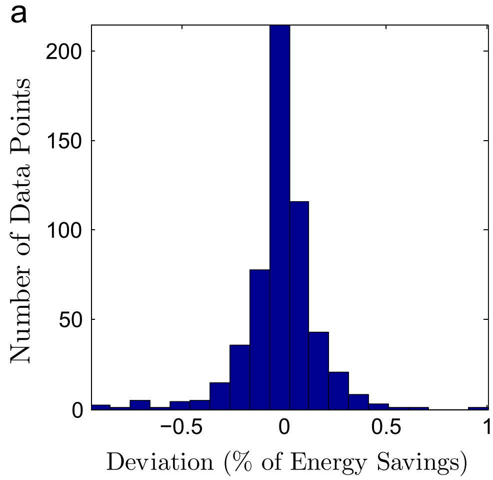

Energy savings.

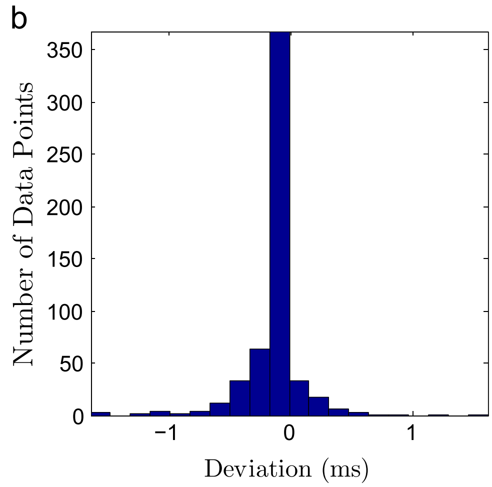

Delay.

Fig. 8. Deviation of theoretical from experimental metrics for the LTE DRX with λ=0.1, b=2.5 ms, $T_\alpha \in [4, 8, 16, 32, 64]$ ms, $N \in [2, 4, 8, 16]$, $T_\beta \in [4, 8, 16, 32, 64, 128, 256]$ ms, $T_{\mathrm{on}} \in [2, 4, 8, 16, 32, 64, 128]$ ms, and $T_\gamma = 2T_\beta$.

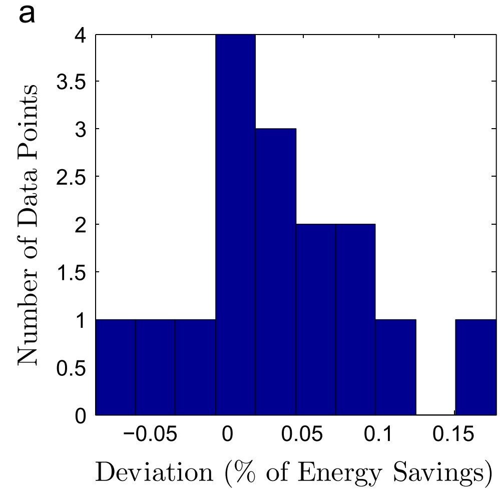

Energy savings.

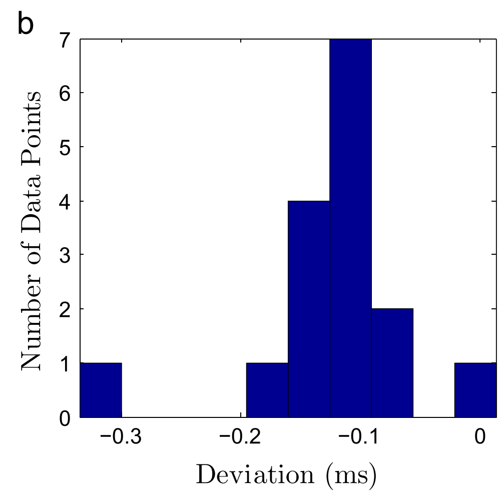

Delay.

Fig. 9. Deviation of theoretical from experimental metrics for LTE DRX with $\lambda = 0.1$, $b = 2.5$ ms, $T_\alpha = 4$ ms, $T_\beta = 4$ ms, $T_{\mathrm{on}} = 2$ ms, $N \in [2, 4, 8, 16]$, and $\frac{T_\gamma}{T_\beta} \in [2, 4, 8, 16, 32]$.

4. Performance evaluation

The focus of this section is to show the validity and accuracy of our modeling approach, and to characterize the benefits provided by our cross-carrier-aware DRX over the classical DRX.

As discussed in Sections 2 and 3, both DRX schemes depends on multiple parameters and on the PMFs for the packet arrival and service time. Hence, varying all parameters and PMFs simultaneously may create a large number of possible combinations. For example, the cross-carrier-aware DRX depends on the five parameters of the anchor CC (Table 4) and the four parameters of the SCell (Table 5), and the packet arrival and service time PMFs for the anchor CC and SCell. Thus, if each parameter and PMF are varied across n different values and distributions, respectively, there would be $O(n^{13})$ possible combinations. For example, for n=6 we have approximately 1.3e10 possible combinations. Even though some of these combinations can be skipped, e.g., when $T_{\mathrm{on}} \geq T_\beta$, the number of valid combinations is still large. While in the classical DRX the number of parameters is less than that of the cross-carrier-DRX, a similar analysis indicates that for n=6, we would have 2.8e5 possible combinations. Hence, for both DRX schemes, rather than varying all parameters and PMFs simultaneously, we fix a set of them while varying the rest.

For analysis of both DRX schemes, we simulated a system consisting of a BS and a UE. The link between them is composed of an anchor CC and an SCell. The BS has an infinite buffer per CC per UE, as typically considered in the literature, where it stores any packet that cannot be immediately sent to the UE since the corresponding CC is in a “sleep” state or the previously buffered packets are being sent. Once the CC is “awake,” the buffered packets are sent by the BS following a First In, First Out (FIFO) scheme. We consider that there is no packet loss or retransmission between the BS and the UE.

4.1. Classical DRX

For the classical DRX discussed in Section 2, it is enough to focus on a single CC, e.g., the anchor CC, since there are no cross-carrier effects. We consider that the number of packets Λ that arrive in a single subframe follows a Poisson distribution with parameter λ. For the service time X, we utilize a modified Poisson distribution:

$$\mathrm{Prob}\{X = k | b\} = (b-1)^{k-1} \frac{e^{-(b-1)}}{(k-1)!}, \quad b > 1; k = 1, 2, 3, \ldots \tag{113}$$

Therefore, $E\{X\} = b$. X can be interpreted as adding 1 to the result of generating a random variable from a Poisson distribution whose

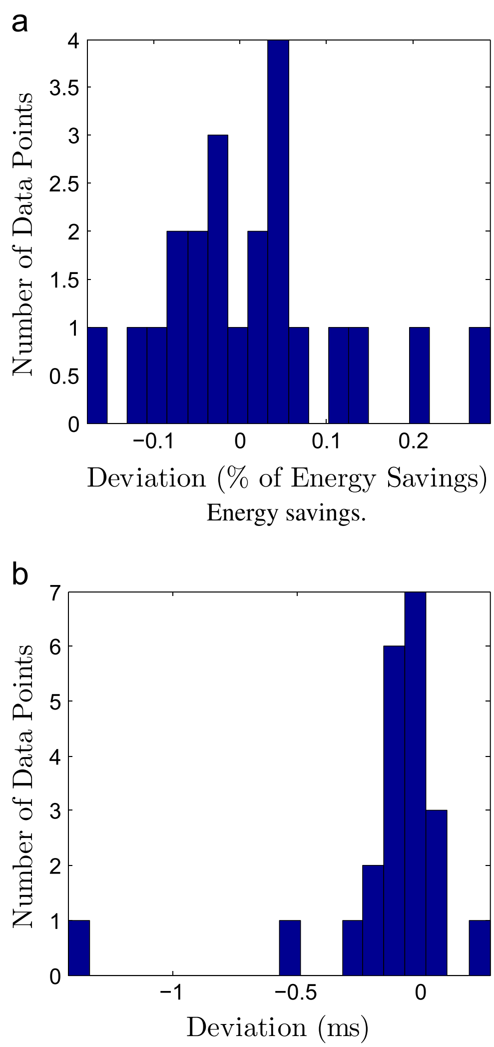

Energy savings.

Delay.

Fig. 10. Deviation of theoretical from experimental metrics for the LTE DRX with $\lambda \in [0.1, 0.05, 0.01, 0.001]$, $b \in [1.5, 2.5, 4.5, 6.5, 8.5, 16.5]$ ms, $T_\alpha = 4$ ms, $T_\beta = 8$ ms, $T_{on} = 2$ ms, $N=2$, and $T_\gamma = 2T_\beta$.

mean is $b-1$. For the classical DRX, the expressions of energy savings and delay utilized here correspond to Eqs. (23) and (30), respectively.

In Fig. 8, we depict the histogram of the deviation between the analytical and simulation results for the energy savings and delay across multiple DRX parameters combinations. For each combination, the operation of the LTE DRX during 1 million subframes was simulated. At the end of each simulation, the energy savings and delay were computed and compared to the results found from the analytical expressions. For each configuration, the deviation is then computed as the difference between the theoretical and simulated performance metrics.

From Fig. 8, we observe that the deviation for both metrics is extremely low. In particular, the absolute deviation in the energy savings is less than 1%. Similarly, the absolute deviation in the delay is mostly within 1 ms. From these results, we validate the significantly high accuracy of the analytical expressions derived for the performance metrics. This validation allows us to further examine the performance metrics, as T_α, N, T_β, and T_{on} are varied, directly through the analytical expressions.

In Fig. 9, we depict the histogram of the deviation between the analytical and simulation results for the energy savings and delay metrics as N and $\frac{T_\gamma}{T_\beta}$ are varied. For each combination of the DRX parameters, the deviation was computed the same way as for Fig. 8. Here, we also have extremely low deviations. In particular, the absolute deviation in the energy savings is less than 0.2%. Similarly, the absolute deviation in the delay is mostly within 0.2 ms. These low levels of deviation allow us to further examine the performance metrics, as N and $\frac{T_\gamma}{T_\beta}$ are varied, directly through the analytical expressions.

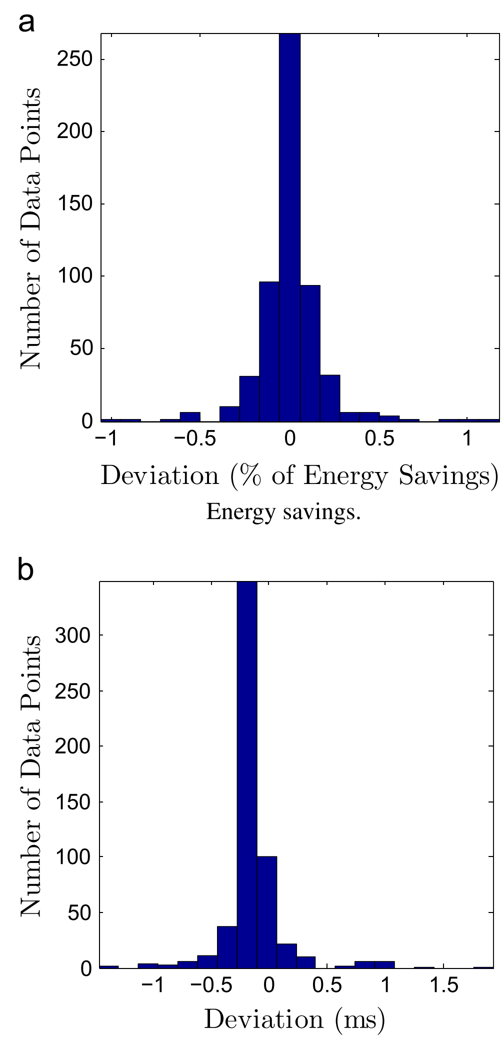

Energy savings.

Delay.

Fig. 11. Deviation of theoretical from experimental metrics for the cross-carrier-aware DRX with parameters $\lambda_1 = 0.1$, $b_1 = 2.5$ ms, $T_{\alpha 1} = 4$ ms, $T_{\beta 1} = 8$ ms, $T_{on1} = 2$ ms, $T_{\gamma 1} = 16$ ms, $N=4$, $\lambda_2 = 0.1$, $b_2 = 2.5$ ms, $T_{\alpha 2} \in [4, 8, 16, 32, 64]$ ms, $T_{\beta 2} \in [4, 8, 16, 32, 64, 128, 256]$ ms, $M \in [2, 4, 8, 16]$, $T_{on2} \in [2, 4, 8, 16, 32, 64, 128]$ ms.

In Fig. 10, we depict the histogram of the deviation between the analytical and simulation results for the energy savings and delay metrics as λ and b are varied. For each combination of the DRX parameters, the deviation was computed as for Fig. 8. Here, we also have extremely low deviations. In particular, the absolute deviation in the energy savings is less than 0.3%. Similarly, the absolute deviation in the delay is mostly within 0.5 ms. These low levels of deviation allow us to further examine the performance metrics, as λ and b are varied, directly through the analytical expressions.

4.2. Cross-carrier-aware DRX

Here, the link between the UE and the BS is composed of an anchor CC and an SCell operating according to our cross-carrier-aware DRX. The number of packets that arrive in a single subframe

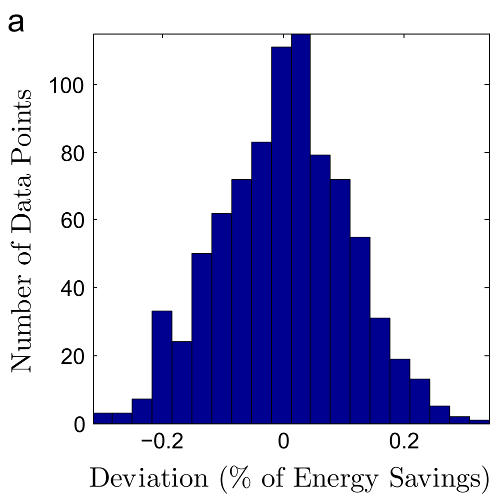

Energy savings.

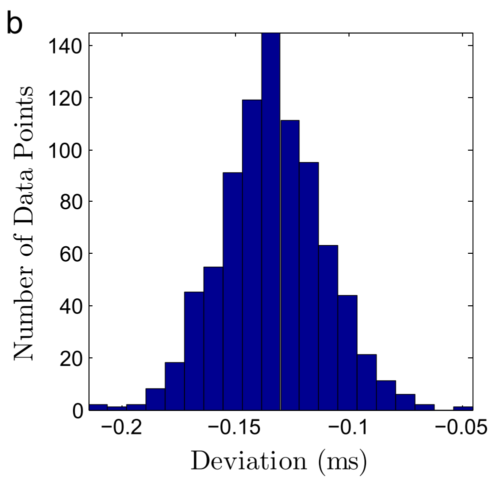

Delay.

Fig. 12. Deviation of theoretical from experimental metrics for the cross-carrier-aware DRX with parameters $\lambda_1 = 0.1$, $T_{\alpha 1} \in [4, 8, 16, 32, 64]$ ms, $b_1 = 2.5$ ms, $T_{\beta 1} \in [4, 8, 16, 3, 64, 128]$ ms, $T_{on1} = [2, 4, 8, 16, 32, 64]$ ms, $T_{\gamma 1} \in [1, 2] T_{\beta 1}$, $N \in [2, 4, 8, 16]$, $\lambda_2 = 0.1$, $b_2 = 2.5$ ms, $T_{\alpha 2} = 4$ ms, $T_{\beta 2} = 32$ ms, $T_{on2} = 16$ ms, and M=2.

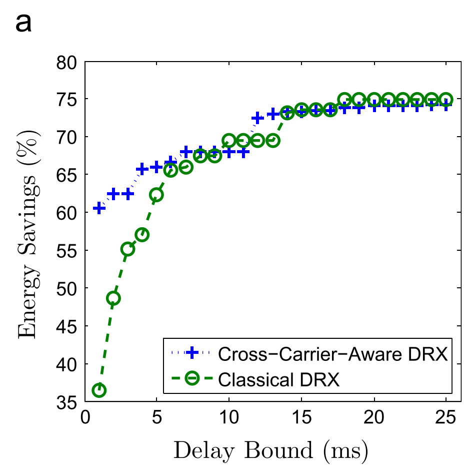

Energy savings.

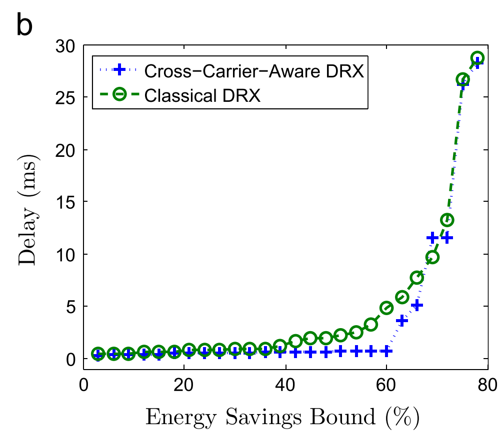

Delay.

Fig. 13. Difference in the performance metrics of the cross-carrier-aware DRX over the classical DRX. SCell parameters $\lambda_2 \in [0.05, 0.1]$, $b_2 = 2.5$ ms, $T_{\alpha 2} \in [4, 8, 16, 32, 64]$ ms, $T_{\beta 2} \in [4, 8, 16, 32, 64, 128, 256]$ ms, $T_{on2} \in [2, 4, 8, 16, 32, 64, 128]$ ms, $M \in [1, 2, 4, 8, 16]$, and for the classical DRX $T_{\gamma 2} = 2T_{\beta 2}$. Anchor CC parameters $\lambda_1 = 0.125$, $b_1 = 2.5$ ms, $T_{\alpha 1} \in [4, 16, 64]$ ms, $T_{\beta 1} \in [4, 32, 256]$ ms, $T_{on1} \in [2, 16, 128]$ ms, N=1, $T_{\gamma 1} = T_{\beta 1}$.

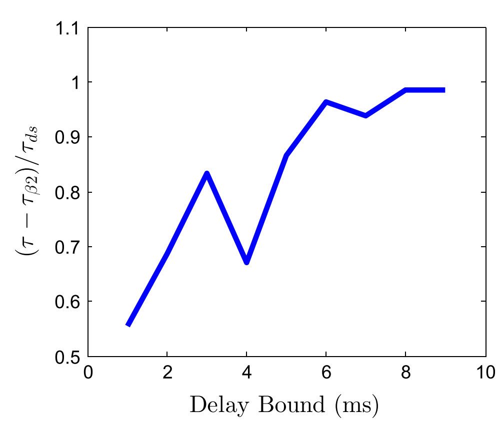

Fig. 14. Factor σ for multiple delay bounds.

for the anchor CC and the SCell are denoted by Λ_1 and Λ_2, respectively, and their means are represented by λ_1 and λ_2. The service times for the anchor CC and the SCell are denoted by X_1 and X_2, respectively, and their means are represented by b_1 and b_2. Λ_1 and Λ_2 are considered to follow a Poisson distribution, and X_1 and X_2 are considered to follow a modified Poisson distribution whose PMF is described by Eq. (113). For the cross-carrier-aware DRX discussed in Section 3 the expressions of energy savings and delay utilized here correspond to Eqs. (105) and (108), respectively.

In Fig. 11, we depict the histogram of the deviation between the analytical and simulation results for the energy savings and delay metrics of the SCell, across multiple SCell DRX parameters. For each combination of those parameters, the operation of the cross-carrier-aware DRX during 1 million subframes was simulated. At the end of each simulation, the energy savings and delay metrics were computed and compared to the results found from the analytical expressions. For each configuration, the deviation is then computed as the difference between the theoretical and simulated performance metrics.

From Fig. 11, we observe that the deviation for both metrics is extremely low. In particular, the absolute deviation in the energy savings is less than 1%. Similarly, the absolute deviation in the delay is mostly within 1ms. From these results, we validate the significantly high accuracy, with respect to the DRX parameters of the SCell, of the analytical expressions derived for the performance metrics of the cross-carrier-aware DRX.

In Fig. 12, we depict the histogram of the deviation between the analytical and simulation results for the energy savings and delay

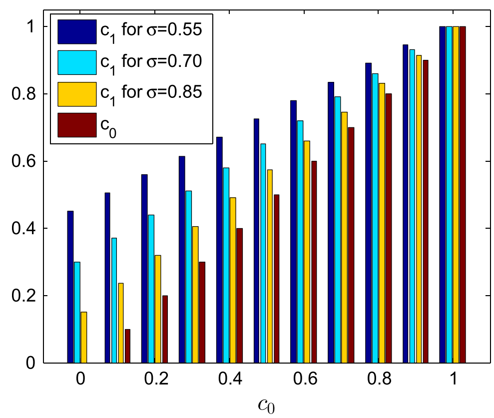

Fig. 15. Comparison of c_1 and c_0 for multiple values of σ.

metrics of the SCell across multiple DRX parameters for the anchor CC. For each combination of those parameters, the deviation is computed as for Fig. 11. Here, we also have extremely low deviations. In particular, the absolute deviation in the energy savings is less than 0.3%. Similarly, the absolute deviation in the delay is less than 0.25 ms. From these results, we validate the significantly high accuracy, also with respect to the DRX parameters of the anchor CC, of the analytical expressions derived for the performance metrics of the cross-carrier-aware DRX.

We now compare the improvements in the performance metrics of the SCell provided by our cross-carrier-aware DRX to those of the classical DRX across multiple DRX parameters by directly using the analytical expressions we have derived. For every possible combination of DRX parameters and a given maximum delay, we compute the highest energy savings provided by the classical and the cross-carrier-aware DRX. Similarly, for minimum energy savings, we compute the minimum delay caused by each of the DRX schemes.

Figure 13a depicts the energy savings provided by our DRX and the classical DRX, while Fig. 13b does a similar comparison for the delay. In Fig. 13a, we observe that our cross-carrier-aware DRX significantly outperforms the classical DRX when the delay limit is less than 5 ms. For a higher delay limit, the difference between the two DRX schemes is very small. However, increasing the energy savings while maintaining a low delay limit is what presents the greatest challenge; thus, the cross-carrier-aware DRX proves to be much more efficient than the classical scheme. In Fig. 13b, we observe that our cross-carrier-aware DRX also outperforms the classical DRX when the energy savings limit is up to 60%. Over the interval of 60–80%, the delay caused by the cross-carrier-aware DRX is not significantly different from that of the classical DRX.

As discussed in Section 3.5.1, the implementation-independent energy savings may differ from the implementation-dependent energy savings particularly when the power consumed $c_0 P_{\max}$ during the traditional "sleep" period is different from that consumed $c_1 P_{\max}$ during the DSS. Nonetheless, we found that if Eq. (107) is satisfied then the implementation-dependent energy savings of the cross-carrier-aware DRX are greater than those of the classical DRX. In Eq. (107), the factor $\sigma \triangleq (\tau - \tau_{\beta 2})/\tau_{\mathrm{ds}}$ plays a key role. Thus, in Fig. 14, we present such factor for the configurations depicted in Fig. 13a for the delay bound less than 10 ms since this is the range where the benefits of our cross-carrier-aware DRX are greater. We observe that σ grows from 0.55 up to 0.99 as the delay bound grows from 1 ms to 9 ms. For three values of σ in such range, we present in Fig. 15 the comparison between c_1 and c_0. For the lowest delay bound, i.e., for $\sigma = 0.55$ and with our algorithm providing the largest improvements, we observe that the value of c_1 can be relatively large compared to c_0, particularly for low values of c_0. A similar behavior is also seen for $\sigma = 0.7$. However, for $\sigma = 0.85$, i.e., when the performance of the classical DRX approaches that of our cross-carrier-aware DRX, we do observe that the values of c_1 are very close to those of c_0. In other words, for the scenarios where the implementation-independent metrics of energy savings are close for both DRX schemes, the values of c_1 and c_0 need to be very similar in order to keep the improvements of our cross-carrier-aware DRX in the implementation-dependent metrics of energy savings. From the previous results, we can state that when $c_1 > c_0$, the implementation-dependent energy savings and the benefits of our cross-carrier-aware DRX can still be greater than the ones of the classical DRX, for a wide range of values for c_1 and c_0.

5. Conclusions

Because of its limited on-board energy, it is critical for the UE to maximize its energy efficiency. With this objective in mind, 3GPP introduced in LTE the use of DRX to minimize the energy consumption at the UE. For scenarios that support CA and MSCA in LTE-A, not only the peak data rate, but also the energy consumption is increased. For such scenarios, the use of DRX still remains the best approach to reducing the UE energy consumption. However, simply using the classical DRX scheme, as is frequently done in the existing literature, leads to high inefficiency. In this paper, we first developed a semi-Markov Chain model to characterize the operation and performance metrics of the classical DRX. Second, we proposed a novel cross-carrier-aware DRX for scenarios that support CA and MSCA. We developed a semi-Markov Chain model and obtained the analytical expressions for the performance metrics for our proposed DRX scheme. The accuracy of analytical expressions was validated through extensive simulations for both DRX schemes. Then, we compared the performance of our cross-carrier-aware DRX against that of the classical DRX. We found that our DRX scheme significantly outperforms the classical DRX in terms of energy savings, especially in the most challenging condition of low tolerable delay. Moreover, the delay caused by our cross-carrier-aware DRX was not found to be significantly different from that of the classical DRX. In addition, we found that our cross-carrier-aware DRX provides benefits over the classical DRX even in non-ideal implementation scenarios.

Acknowledgments

This project was funded by the Deanship of Scientific Research (DSR), King Abdulaziz University, under Grant no. (3-611-35-HiCi). The authors, therefore, acknowledge technical and financial support of KAU. In addition, this work was partly supported by the Secretaría Nacional de Ciencia y Technología (SENACYT), Republic of Panama.

References

3GPP. Radio Link Control (RLC) protocol specification. Technical Specification 36.322; September 2010.
3GPP. Evolved universal terrestrial radio access (E-UTRA), LTE physical layer, General description. Technical Specification 36.201; March 2011.
3GPP. Medium access control (MAC) protocol specification. Technical Specification 36.321; March 2013.
3GPP. Packet data convergence protocol (PDCP) specification. Technical Specification 36.323; March 2013.
3GPP. Evolved universal terrestrial radio access (E-UTRA), Physical layer procedures. Technical Specification 36.213; March 2014.
3GPP. Radio resource control (RRC), Protocol specification. Technical Specification 36.331; June 2014.

Akyildiz IF, Gutierrez-Estevez DM, Balakrishnan R, Chavarria-Reyes E. LTE-Advanced and the evolution to Beyond 4G (B4G) systems. Phys Commun J (Elsevier) 2014;10(0):31–60.

Bontu C, Illidge E. DRX mechanism for power saving in LTE. IEEE Commun Mag 2009;47(June (6)):48–55.

Jha S, Koc A, Vannithamby R, Torlak M. Adaptive DRX configuration to optimize device power saving and latency of mobile applications over LTE advanced network. In: Proceedings of the IEEE international conference on communications (ICC); 2013. p. 6210–4.

Jin S, Qiao D. Numerical analysis of the power saving in 3GPP LTE advanced wireless networks. 2012;61(4):1779–85.

Koc A, Jha S, Vannithamby R, Torlak M. Device power saving and latency optimization in LTE-A networks through DRX configuration; 2014.

Lee T-H, Tsai C-J, Wu T-H. Quality of service support under DRX mechanism in LTE advanced wireless networks. In: Proceedings of the IEEE vehicular technology conference (VTC); 2013. p. 1–5.

Takagi H. Queueing analysis: a foundation of performance evaluation, vol. 3. Amsterdam, New York: Elsevier Science Publishers B.V.; 1993.

Wang H-C, Tseng C-C, Chen G-Y, Kuo F-C, Ting K-C. Accurate analysis of delay and power consumption of LTE DRX mechanism with a combination of short and long cycles. In: Proceedings of the international symposium on wireless personal multimedia communications (WPMC); 2012. p. 384–88.

Zhang YF, Gao ST, Tian H, Huang B. Delay analysis of DRX in LTE-advanced considering carrier aggregation. J China Univ Posts Telecommun 2011;18(December (6)):1–7.

Zhong C, Yang T, Zhang L, Wang J. A new discontinuous reception (DRX) scheme for LTE-advanced carrier aggregation systems with multiple services. In: Proceedings of the IEEE vehicular technology conference (VTC); September 2011. p. 1–5.

Zhou L, Xu H, Tian H, Gao Y, Du L, Chen L. Performance analysis of power saving mechanism with adjustable DRX cycles in 3GPP LTE. In: Proceedings of the IEEE vehicular technology conference (VTC); 2008. p. 1–5.

Zhou K, Nikaein N, Spyropoulos T. LTE/LTE-a discontinuous reception modeling for machine type communications. IEEE Wirel Commun Lett 2013;2(February (1)):102–5.